Synthesis, Molecular Structure, and Solution Stereochemistry of Hypercoordinated Bis(3-(dimethylamino)propyl)tin Compounds. Dissociative (Nonregular) and Nondissociative (Regular) Isomerization Pathways†

Klaus Jurkschat,*,‡ Nicole Pieper, Stefan Seemeyer, and Markus Schürmann

Universität Dortmund, Lehrstuhl für Anorganische Chemie II, D-44221 Dortmund, Germany

Monique Biesemans, Ingrid Verbruggen, and Rudolph Willem*

High-Resolution NMR Centre (HNMR), Free University of Brussels (VUB), Pleinlaan 2, B-1050 Brussel, Belgium

Received September 21, 2000

The syntheses of $[Me_2N(CH_2)_3]_2Sn(EAr)_2$ (**1**, E = O, Ar = C_6H_5; **2**, E = O, Ar = p-*t*-BuC_6H_4; **3**, E = O, Ar = p-$NO_2C_6H_4$; **4**, E = O, Ar = o-FC_6H_4; **7**, E = S, Ar = C_6H_5), $[Me_2N(CH_2)_3]_2$-Sn(*o*-$O_2C_6H_3$R-3) (**5**, R = H; **6**, R = OCH_3), and $\{[Me_2N(CH_2)_3]_2SnPh\}^+I^-$ (**8**) are reported. X-ray diffraction analyses reveal distorted-octahedral geometries for the tin atoms in compounds **1**−**7** with, except for the stannaindane derivative **5**, the carbon atoms in mutually *trans* positions, while the nitrogen and oxygen atoms are *cis*. In compound **5**, the carbon atoms are *cis*, whereas the nitrogen atoms are *trans*. Compound **8**, in contrast, is ionic and consists of an intramolecularly pentacoordinated triorganotin cation and an iodide anion. Variable-temperature ^1H, ^{13}C, and ^{119}Sn NMR investigations reveal the compounds to have similar structures in solution. The coalescence phenomena observed in the ^1H and ^{13}C NMR spectra are explained both in terms of Sn−O bond cleavage (**1**−**4**) and chirality inversion through a sequence of five intramolecular Berry-type pseudorotations (**1**−**4**, **8**), interconverting the enantiomers with propeller-like geometry. The dynamic behavior in solution of the stannaindane derivatives **5** and **6** and of the thiophenolate derivative **7** is interpreted in terms of intramolecular Sn−N bond dissociation.

Introduction

The ability of heavier main-group elements to accommodate more than eight electrons in their valence shell and to form so-called hypervalent or hypercoordinated compounds is well-established, and the chemistry of such compounds in all its different facets has been regularly reviewed over the years.[1] Tin is one of the elements in the center of these investigations, and there is a plethora of compounds in which tin expands its coordination number to 5, 6, or 7.[2] Prominent representatives of five- and six-coordinate organotin compounds are those containing intramolecularly coordinating C,Y-chelating ligands (Y = heteroatom-containing substituent).[2−6] Among these, especially chiral pentacoordinated derivatives have stirred increasing interest as reagents in organic synthesis, and this is associated with both their enhanced reactivity and configurational stability.[7] Consequently, the static and dynamic stereochemistry in solution of five-coordinate compounds has been intensively studied[3a] and dissociative (nonregular)[3a] as well as nondissociative (regular)[8] mechanisms have been proposed to account for the coalescence phenomena observed for their temperature-dependent NMR spectra. In contrast, much less is known on the stereochemistry of related intramolecularly hexacoordinated organotin compounds containing two C,Y-chelating ligands.[6e,f,9] Thus, in 1979 van Koten and co-workers interpreted results from temperature-dependent proton spectra for $(2\text{-}Me_2NCH_2C_6H_4)_2SnBr_2$ in terms of Sn−N bond dissociation, with, however, the propeller chirality of the

† This work contains part of the Ph.D. thesis of N.P., Dortmund University, 1998, and of the intended Ph.D. thesis of S.S.

‡ Fax: 49-231-7555048. E-mail: kjur@platon.chemie.uni-dortmund.de.

(1) (a) Akiba, K., Ed. *Chemistry of Hypervalent Compounds*; Wiley-VCH: Weinheim, Germany, 1999, and references therein. (b) Holmes, R. R. *Chem. Rev.* **1990**, *90*, 17. (c) Corriu, R. J. P.; Chuit, C.; Reye, C.; Young, J. C. *Chem. Rev.* **1993**, *93*, 1371.

(2) Smith, P. J., Ed. *Chemistry of Tin*; Blackie Academic & Professional: Glasgow, U.K., 1998.

(3) (a) Jastrzebski, J. T. B. H.; Van Koten, G. *Adv. Organomet. Chem.* **1993**, *35*, 241 and references therein. (b) Jastrzebski, J. T. B. H.; Grove, D. M.; Boersma, J.; Van Koten, G.; Ernsting, J.-M. *Magn. Reson. Chem.* **1991**, *29*, S25 and references therein.

(4) (a) Kolb, U.; Dräger, M.; Dargatz, M.; Jurkschat, K. *Organometallics* **1995**, *14*, 2827. (b) Hoppe, S.; Weichmann, H.; Jurkschat, K.; Schneider-Koglin, C.; Dräger, M. *J. Organomet. Chem.* **1995**, *505*, 63. (c) Pieper, N.; Klaus-Mrestani, C.; Schürmann, M.; Jurkschat, K.; Biesemans, M.; Verbruggen, I.; Martins, J.; Willem, R. *Organometallics* **1997**, *16*, 1043. (d) Dakternieks, D.; Jurkschat, K.; Tozer, R.; Hook, J.; Tiekink, E. R. T. *Organometallics* **1997**, *16*, 3696. (e) Zickgraf, A.; Beuter, M.; Kolb, U.; Dräger, M.; Tozer, R.; Dakternieks, D.; Jurkschat, K. *Inorg. Chim. Acta* **1998**, *275*−*276*, 203. (f) Mehring, M.; Schürmann, M.; Jurkschat, K. *Organometallics* **1998**, *17*, 1227. (g) Mehring, M.; Löw, C.; Schürmann, M.; Jurkschat, K. *Eur. J. Inorg. Chem.* **1999**, 887. (h) Pieper, N.; Ludwig, R.; Schürmann, M.; Jurkschat, K.; Biesemans, M.; Verbruggen, I.; Willem, R. *Phosphorus, Sulfur Silicon Relat. Elem.* **1999**, *150*−*151*, 305.

10.1021/om000813w CCC: $20.00
Publication on Web 02/03/2001

molecule being preserved at high temperature.[9] Later on, this view got further support by the rigidity of related $[8\text{-}Me_2N\text{-}1\text{-}C_{10}H_6]_2SnBr_2$, in which the dimethylamino groups are prevented from Sn−N dissociation.[10] For the intramolecularly hexacoordinated triorganotin iodide $[8\text{-}Me_2N\text{-}1\text{-}C_{10}H_6]_2SnIMe$ no unambiguous distinction was made between dissociative and nondissociative mechanisms to account for the coalescence phenomena observed in the temperature-dependent ^1H, ^{13}C, and ^{119}Sn NMR spectra.[11]

In a previous paper we reported the synthesis and dynamic stereochemistry in solution of the intramolecularly hexacoordinated diorganotin difluoride $[Me_2N(CH_2)_3]_2SnF_2$.[4c] In the solid state, the compound, as its water adduct, contains a hexacoordinated tin with the carbon, nitrogen, and fluorine atoms being mutually *trans*. In solution, however, there is an equilibrium between *cis* and *trans* isomers. Interestingly, this equilibrium proceeds through intermolecular fluoride exchange rather than through intramolecular Sn−N bond dissociation. This result was somewhat unexpected and was in striking contrast with the Sn−N bond dissociation proposed to be responsible for the enantiomerization of $(2\text{-}Me_2NCH_2C_6H_4)_2SnBr_2$.[9]

In this paper we investigate the phenolate and thiophenolate derivatives $[Me_2N(CH_2)_3]_2Sn(EAr)_2$ (**1**, E = O, Ar = C_6H_5; **2**, E = O, Ar = p-*t*-BuC_6H_4; **3**, E = O, Ar = p-$NO_2C_6H_4$; **4**, E = O, Ar = o-FC_6H_4; **7**, E = S, Ar = C_6H_5), the stannaindane derivatives $[Me_2N(CH_2)_3]_2Sn(o\text{-}O_2C_6H_3R\text{-}3)$ (**5**, R = H; **6**, R = OCH_3), and the triorganotin cation $\{[Me_2N(CH_2)_3]_2SnPh\}^+I^-$ (**8**). We show that the enantiomerization of intramolecularly hexacoordinated organotin compounds involves the formation of pentacoordinated intermediates which in turn undergo either Berry-type pseudorotations or dissociative mechanisms, depending on the peculiar structural features of the compounds **1**−**8**.

Results and Discussion

Synthetic Aspects. The bis(3-(dimethylamino)propyl)tin diphenolate derivatives **1**−**4** were synthesized in good to moderate yields by heating at reflux a solution of bis(3-(dimethylamino)propyl)diphenyltin[4c] and the corresponding substituted phenols in toluene (eq 1). In

$$[Me_2N(CH_2)_3]_2SnPh_2 + 2ArOH \xrightarrow[-2C_6H_6]{\text{toluene, 6.5 h, reflux}} [Me_2N(CH_2)_3]_2Sn(OAr)_2 \quad (1)$$

1−**4**

1, Ar = C_6H_5
2, 4-*t*-BuC_6H_4
3, 4-$NO_2C_6H_4$
4, 2-FC_6H_4

a similar manner, the reaction of bis(3-(dimethylamino)-propyl)diphenyltin with the corresponding catechols afforded the 2,2-bis(3-(dimethylamino)propyl)-1,3-dioxa-2-stannaindanes **5** and **6** (eq 2). These reactions are

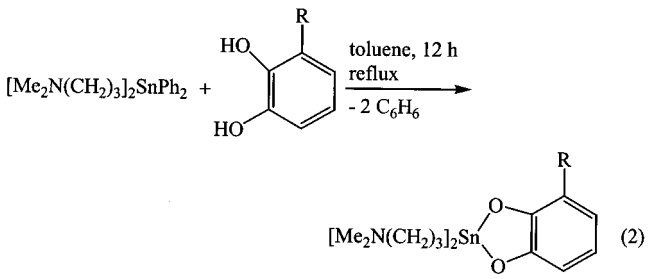

(2)

5, R = H
6, R = OCH_3

further examples of intramolecularly donor-assisted enhanced Sn−C reactivity.[10]

Reacting the diorganotin diphenolate **1** with thiophenol provided bis(3-(dimethylamino)propyl)tin dithiophenolate (**7**) in good yield (eq 3). The reaction of bis(3-(dimethylamino)propyl)diphenyltin with 1 molar equiv of iodine proceeds with selective cleavage of one tin−phenyl bond and afforded almost quantitatively the intramolecularly coordinated triorganotin iodide **8** (eq 4). Compounds **1**−**4**, **7**, and **8** are colorless crystalline solids, whereas **5** and **6** are violet crystals. They are readily soluble in common organic solvents such as chloroform, dichloromethane, and tetrahydrofurane.

$$[Me_2N(CH_2)_3]_2Sn(OPh)_2 + 2PhSH \xrightarrow[-2PhOH]{\text{toluene, 12 h, reflux}} [Me_2N(CH_2)_3]_2Sn(SPh)_2 \quad (3)$$

1 **7**

$$[Me_2N(CH_2)_3]_2SnPh_2 + I_2 \xrightarrow[-PhI]{CH_2Cl_2} \{[Me_2N(CH_2)_3]_2SnPh\}^+I^- \quad (4)$$

8

(5) (a) Willem, R.; Delmotte, A.; De Borger, I.; Biesemans, M.; Gielen, M.; Kayser, F. *J. Organomet. Chem.* **1994**, *480*, 255. (b) Kayser, F.; Biesemans, M.; Delmotte, A.; Verbruggen, I.; De Borger, I.; Gielen, M.; Willem, R.; Tiekink, E. R. T. *Organometallics* **1994**, *13*, 4026. (c) Biesemans, M.; Willem, R.; Damoun, S.; Geerlings, P.; Lahcini, M.; Jaumier, P.; Jousseaume, B. *Organometallics* **1996**, *15*, 2237. (d) Biesemans, M.; Willem, R.; Damoun, S.; Geerlings, P.; Tiekink, E. R. T.; Jaumier, P.; Lahcini, M.; Jousseaume, B. *Organometallics* **1998**, *17*, 90. (e) Susperregui, J.; Bayle, M.; Leger, J. M.; Deleris, G.; Biesemans, M.; Willem, R.; Kemmer, M.; Gielen, M. *J. Organomet. Chem.* **1997**, *545*−*546*, 559. (f) Willem, R.; Biesemans, M.; Jaumier, P.; Jousseaume, B. *J. Organomet. Chem.* **1999**, *572*, 233. (g) Martins, J.; Biesemans, M.; Willem, R. *Prog. NMR Spectrosc.* **2000**, *36*, 271.

(6) (a) Dostal, S.; Stoudt, S. J.; Fanwick, P.; Sereatan, F.; Kahr, B.; Jackson, E. *Organometallics* **1993**, *12*, 2284. (b) Dölling, K.; Krug, A.; Hartung, H.; Weichmann, H. *Z. Anorg. Allg. Chem.* **1995**, *621*, 63. (c) Balasubramanian, R.; Chohan, Z. H.; Doidge-Harrison, S. M. S. V.; Howie, R. A.; Wardell, J. L. *Polyhedron* **1997**, *16*, 4283. (d) Rippstein, R.; Kickelbick, G.; Schubert, U. *Monatsh. Chem.* **1999**, *130*, 385. (e) Ovchinnikov, Y. E.; Podozhikh, S. A.; Razumovskaya, I. V.; Bylikin, S. Y.; Shipov, A. G.; Smirnova, L. S.; Negrebetsky, V. V.; Baukov, Y. I. *Russ. Chem. Bull.* **1999**, *48*, 1964. (f) Bylikin, S. Y.; Podozhikh, S. A.; Shipov, A. G.; Negrebetsky, V. V.; Ovchinnikov, Y. E.; Baukov, Y. I. *Russ. Chem. Bull.* **2000**, *49*, 755.

(7) (a) Schwartzkopf, K.; Blumenstein, M.; Hayen, A.; Metzger, J. O. *Eur. J. Org. Chem.* **1998**, *177*, 7. (b) Schumann, H.; Wassermann, B. C.; Hahn, F. E. C. *Organometallics* **1992**, *11*, 2803. (c) Dakternieks, D.; Dunn, K.; Perchyonok, V. T.; Schiesser, C. H. *Chem. Commun.* **1999**, 1665.

(8) (a) Colton, R.; Dakternieks, D. *Inorg. Chim. Acta* **1985**, L17. (b) Jurkschat, K.; Kalbitz, J.; Dargatz, M.; Kleinpeter, E.; Tzschach, A. *J. Organomet. Chem.* **1988**, *347*, 41.

(9) Van Koten, G.; Jastrzebski, J. T. B. H.; Noltes, J. G. *J. Organomet. Chem.* **1979**, *177*, 283.

(10) (a) Jastrzebski, J. T. B. H.; Van der Schaaf, P. A.; Boersma, J.; Van Koten, G.; de Wit, M.; Wang, Y.; Heijdenrijk, D.; Stam, C. H. *J. Organomet. Chem.* **1991**, *401*, 301. (b) Dakternieks, D.; Dyson, G.; Jurkschat, K.; Tozer, R.; Tiekink, E. R. T. *J. Organomet. Chem.* **1993**, *458*, 29.

(11) Jastrzebski, J. T. B. H.; Van der Schaaf, P. A.; Boersma, J.; Van Koten, G.; de Ridder, D. J. A.; Heijdenrijk, D. *Organometallics* **1992**, *11*, 1521.

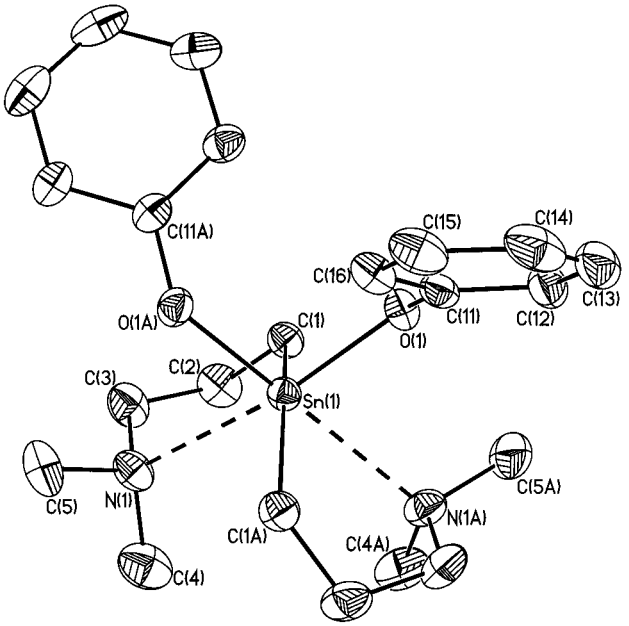

Figure 1. General view (SHELXTL) of a molecule showing 30% probability displacement ellipsoids and the atom numbering (symmetry transformations used to generate equivalent atoms: A, 0.5 − *x*, 0.5 − *y*, *z*) for **1**.

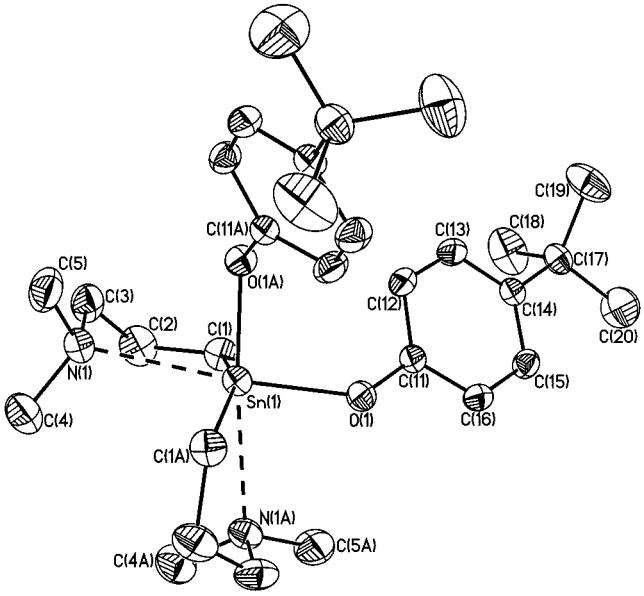

Figure 2. General view (SHELXTL) of a molecule showing 30% probability displacement ellipsoids and the atom numbering (symmetry transformations used to generate equivalent atoms: A, −*x*, *y*, 0.5 − *z*) for **2**.

Molecular Structures of the Diorganotin Diphenolate Derivatives 1−4, the Diorganotin Dithiophenolate Derivative 7, and the Triorganotin Cation 8. The molecular structures of compounds **1**−**4**, **7**, and **8** are shown in Figures 1−6. The crystallographic data are given in Table 1, and selected bond lengths and bond angles are summarized in Table 2.

The tin atoms in **1**−**4** and **7** are each six-coordinated by two carbons, two oxygens, and two nitrogens, with an overall distorted-octahedral *trans*−*cis*−*cis* configuration. The 12 *cis* angles average 92.3° (76.8(1)−103.9(2)°) for **1**, 92.3° (76.0(7)−104.1(8)°) for **2**, 90.7° (76.9(8)−106.2(1)°) for **3**, 91.8° (77.9(9)−104.5(1)°) for **4**, and 91.3° (73.0(1)−104.0(9)°) for **7**. The distortion from the ideal octahedral geometry is especially apparent in the C(1)−Sn−C(1a) angles, which fall in the range from 161.8(1)° (**3**) to 144.58(17)° (**7**). The configuration of the tin atoms in these compounds resembles that of the tin atoms in $(MeO_2CCH_2CH_2)_2SnX_2$ (X = Cl, Br, I)[6c] and $\{[Me_2N(CH_2)_3]_2SnS\}_2$,[12] but the octahedral geometry of the latter compound with a C−Sn−C angle of 137.2(2)° is even more distorted. In contrast, the related compounds $[Me_2N(CH_2)_3]_2SnCl_2$,[13] $(Me_2NCH_2CH_2CMe_2)_2SnCl_2$,[13] and $[Me_2N(CH_2)_3]_2SnF_2{\cdot}2H_2O$[4c] all display a mutually *trans* configuration in the solid state.

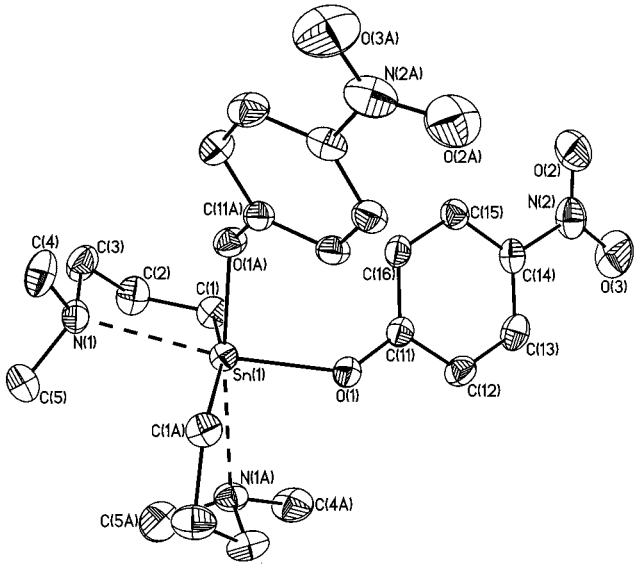

Figure 3. General view (SHELXTL) of a molecule showing 30% probability displacement ellipsoids and the atom numbering (symmetry transformations used to generate equivalent atoms: A, −*x*, −*y*, *z*) for **3**.

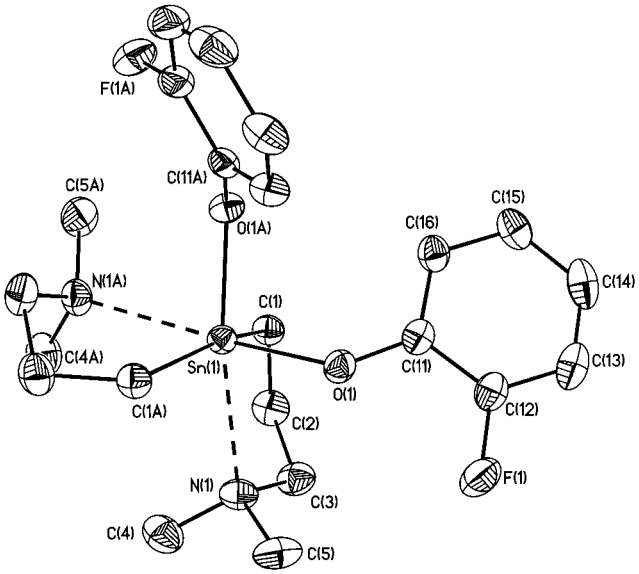

Figure 4. General view (SHELXTL) of a molecule showing 30% probability displacement ellipsoids and the atom numbering (symmetry transformations used to generate equivalent atoms: A, 1 − *x*, −*y*, *z*) for **4**.

(12) Jurkschat, K.; Van Dreumel, S.; Dyson, G.; Dakternieks, D.; Bastow, T. J.; Smith, M. E.; Dräger, M. *Polyhedron* **1992**, *11*, 2747.
(13) Schollmeyer, D.; Hartung, H.; Klaus, C.; Jurkschat, K. *Main Group Met. Chem.* **1991**, *14*, 27.

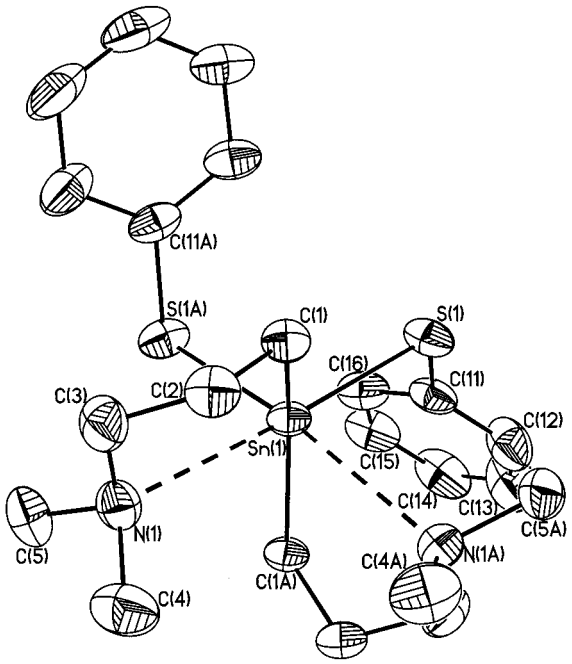

Figure 5. General view (SHELXTL) of a molecule showing 30% probability displacement ellipsoids and the atom numbering (symmetry transformations used to generate equivalent atoms: a, $-x$, y, $0.5 - z$) for **7**.

In analogy with $\{[Me_2N(CH_2)_3]_2SnS\}_2$[12] as well as in view of the long Sn−N bond distances between 2.575(2) Å (**3**) and 2.908(3) Å (**7**), the tin atoms in these compounds can also be viewed as [4 + 2]-coordinate; i.e., they represent model compounds along the path tetrahedron−octahedron. The two carbons and the two oxygens (**1**−**4**) or the two sulfurs (**7**) define a distorted tetrahedron, which underlies a *cis* attack by two nitrogens. In contrast to $\{[Me_2N(CH_2)_3]_2SnS\}_2$[12] this *cis* attack is synchronous in **1**−**4** as well as in **7**. The Sn−N distances in the diorganotin diphenolate derivatives **1**−**4** of 2.575(2)−2.670(2) Å are comparable with those found in $[Me_2N(CH_2)_3]_2Sn(OSiPh_2)_2O$ (2.621(4)/2.638(5) Å)[14] but they are longer than in the pentacoordinated phenolate $[Me_2N(CH_2)_3]SnPh_2(OPh)$ (2.569(2) Å)[4e] and even much longer than in $[Me_2N(CH_2)_3]_2SnF_2{\cdot}2H_2O$ (2.366(8) Å).[4c] The Sn−N distance of 2.908(3) Å in the diorganotin dithiophenolate **7** is rather long and lies between the Sn−N distances of 2.810(3) and 3.158(5) Å, as measured for the related $\{[Me_2N(CH_2)_3]_2SnS\}_2$.[12]

The triorganotin iodide derivative **8** consists of an intramolecularly coordinated triorganotin cation and an iodide anion which are separated by 4.457(1) Å, a distance slightly larger than the sum of the van der Waals radii of tin (2.20 Å) and iodine (2.15 Å). The tin atom is essentially pentacoordinated with the carbon atoms C(1), C(11), and C(21) occupying the equatorial positions and the nitrogen atoms N(1) and N(2) occupying the axial positions of a slightly distorted trigonal bipyramid. The distortion is manifested in (i) the deviation of the N(1)−Sn(1)−N(2) angle (174.6(2)°) from the ideal value of 180° and (ii) the equatorial C(1)−Sn(1)−C(11), C(1)−Sn(1)−C(21), and C(11)−Sn(1)−C(21) angles of 113.1(2), 115.2(2), and 131.7(2)° differing from 120°. The tin atom is displaced by 0.020(3) Å from the plane defined by C(1), C(11), and C(21) in the direction of N(2). Although, as mentioned above, the Sn(1)···I(1) distance exceeds the sum of the van der Waals radii of tin and iodine, the iodide appears to induce the opening of the C(11)−Sn(1)−C(21) angle. The same holds for the related triorganotin bromide derivative $\{[Me_2N(CH_2)_3]_2SnPh\}^+Br^-$ (**8a**) (Sn···Br = 4.0496(8) Å, C(11)−Sn(1)−C(21) = 132.7(3)°), whereas in the hexafluorophosphate derivative $\{[Me_2N(CH_2)_3]_2SnPh\}^+PF_6^-$ (**8b**) the C(11)−Sn(1)−C(21) angle amounts to 120.9(3)°. Detailed information on compounds **8a** and **8b** will be reported in a forthcoming paper. In fact, the structure of compound **8** can be interpreted as a model for a nucleophilic edge attack of iodide at a pentacoordinated triorganotin cation. It is of particular interest to compare the structure of compound **8** with its closely related intramolecularly hexacoordinated triorganotin iodide $[8\text{-}Me_2N\text{-}1\text{-}C_{10}H_6]_2SnIMe$.[11] The geometry at tin of this compound was interpreted in terms of a nucleophilic edge attack of one nitrogen atom (Sn···N = 3.10(1) Å) on a trigonal bipyramid composed of three carbon atoms in equatorial positions and the other nitrogen (Sn−N = 2.53(1) Å) and the iodide (Sn−I = 2.950(2) Å) in axial positions. The origin of the different structures of the triorganotin cation **8** and the latter compound is not clear yet but might be traced to the $(sp^3\text{-}C)_2(sp^2\text{-}C)SnI$ versus $(sp^3\text{-}C)(sp^2\text{-}C)_2SnI$ substituent patterns of **8** and $[8\text{-}Me_2N\text{-}1\text{-}C_{10}H_6]_2SnIMe$, respectively.

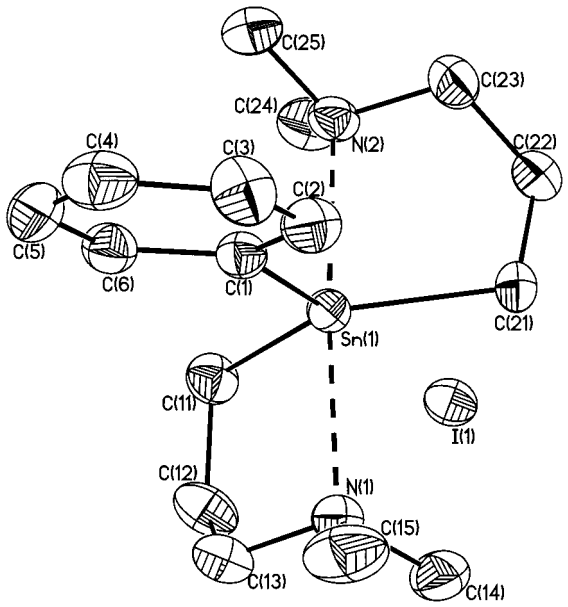

Figure 6. General view (SHELXTL) of a molecule showing 30% probability displacement ellipsoids and the atom numbering for **8**.

The intramolecular Sn−N distances in **8** of 2.392(4) and 2.401(4) Å are far shorter than those in the phenolate derivatives **1**−**4** and the methoxy-substituted stannaindane derivative **6**, but they are close to the distances measured for the stannaindane derivative **5** and the diorganotin difluoride $[Me_2N(CH_2)_3]_2SnF_2{\cdot}2H_2O$.[4c]

The nonequivalence in the triorganotin cation **8**, as shown by the crystal structure, of the four methyl groups, of the six methylene carbons, and of the six phenyl carbons is nicely reflected by the corresponding number of resonances in the ^{13}C CP-MAS NMR spec-

(14) Beckmann, J.; Jurkschat, K.; Kaltenbrunner, U.; Pieper, N.; Schürmann, M. *Organometallics* **1999**, *18*, 1586.

Table 1. Crystallographic Data for 1−8

	1	2	3	4	5	6	7	8
formula	$C_{22}H_{34}N_2O_2Sn$	$C_{30}H_{50}N_2O_2Sn$	$C_{22}H_{32}N_4O_6Sn$	$C_{22}H_{32}F_2N_2O_2Sn$	$C_{16}H_{28}N_2O_2Sn$	$C_{17}H_{30}N_2O_3Sn$	$C_{22}H_{34}N_2S_2Sn$	$[C_{16}H_{29}N_2Sn]^+[I]^-$
fw	477.20	589.41	567.21	513.19	399.09	429.12	509.32	495.00
cryst syst	orthorhombic	monoclinic	orthorhombic	orthorhombic	triclinic	monoclinic	monoclinic	monoclinic
cryst size, mm	0.40 × 0.30 × 0.30	0.25 × 0.15 × 0.15	0.18 × 0.15 × 0.15	0.25 × 0.23 × 0.10	0.24 × 0.08 × 0.08	0.20 × 0.17 × 0.15	0.20 × 0.13 × 0.12	0.15 × 0.13 × 0.13
space group	*Fdd*2	*C*2/*c*	*Fdd*2	*Fdd*2	$P\bar{1}$	$P2_1/c$	C2/*c*	*Cc*
a, Å	13.267(1)	25.123(1)	22.525(1)	13.468(1)	8.779(1)	18.187(1)	22.710(1)	13.360(1)
b, Å	35.456(1)	9.222(1)	23.433(1)	35.097(1)	8.773(1)	13.247(1)	8.844(1)	12.931(1)
c, Å	9.389(1)	16.935(1)	9.371(1)	9.469(1)	11.689(1)	18.365(1)	14.406(1)	11.555(1)
α, deg					77.018(1)			
β, deg		129.108(1)			86.018(1)	118.339(1)	123.19(3)	102.825(1)
γ, deg					81.994(1)			
V, Å^3	4416.5(6)	3044.5(4)	4946.3(6)	4475.9(6)	868.03(16)	3894.3(4)	2421.4(11)	1946.4(3)
Z	8	4	8	8	2	8	4	4
ρ_{calcd}, Mg/m^3	1.435	1.286	1.523	1.523	1.527	1.464	1.397	1.689
μ, mm^{-1}	1.175	0.866	1.077	1.178	1.478	1.327	1.237	2.894
F(000)	1968	1240	2320	2096	408	1760	1048	968
θ range, deg	4.82−25.65	3.10−27.51	3.48−27.55	3.15−27.47	3.01−25.34	2.97−25.42	3.36 to 27.47	3.63 to 25.69
index ranges	$-16 \le h \le 16$	$-32 \le h \le 32$	$-29 \le h \le 29$	$-17 \le h \le 17$	$-10 \le h \le 10$	$-21 \le h \le 21$	$0 \le h \le 29$	$-16 \le h \le 16$
	$-42 \le k \le 42$	$-11 \le k \le 11$	$-29 \le k \le 30$	$-45 \le k \le 45$	$-10 \le k \le 10$	$-16 \le k \le 16$	$0 \le k \le 11$	$-15 \le k \le 15$
	$-11 \le l \le 11$	$-20 \le l \le 17$	$-12 \le l \le 12$	$-12 \le l \le 12$	$-11 \le l \le 12$	$-22 \le l \le 19$	$-18 \le l \le 15$	$-11 \le l \le 11$
no. of rflns collcd	13360	19593	15829	13257	9964	44614	2846	12994
completeness to θ_{max}	99.2	98.5	99.3	99.9	93.0	93.6	99.8	91.7
no. of indep rflns/R_{int}	2024/0.044	3439/0.041	2780/0.033	2504/0.037	2952/0.031	6710/0.043	2779/0.0185	3320/0.021
no. of rflns obsd with $I > 2\sigma(I)$	1688	2512	2356	1972	2568	3620	2349	3132
abs cor T_{max}/T_{min}	not measd	not measd	not measd	not measd	not measd	not measd	ψ scan, 1.000/0.898	not measd
no. of refined params	126	166	154	136	196	427	155	188
GOF (F^2)	0.955	0.918	0.958	0.933	0.999	0.882	1.035	1.040
R1(F) ($I > 2\sigma(I)$)	0.0240	0.0294	0.0214	0.0235	0.0214	0.0296	0.0352	0.0209
wR2(F^2) (all data)	0.0460	0.0549	0.0438	0.0414	0.0476	0.0503	0.0944	0.0488
abs struct param	0.52(2)		0.43(2)	0.51(2)				0.48(2)
extinction coeff								0.0029(2)
$(\Delta/\sigma)_{max}$	<0.001	<0.001	<0.001	<0.001	<0.001	0.001	<0.001	<0.001
largest diff peak/hole, e/Å^3	0.222/−0.476	0.482/−0.305	0.384/−0.385	0.387/−0.338	0.551/−0.310	0.348/−0.340	0.534/−0.584	0.341/−0.351

trum, with the exception that the two $SnCH_2$ resonances are superimposed to give a somewhat broader signal.

Solution Stereochemistry of $[Me_2N(CH_2)_3]_2Sn(OPh)_2$ (1), Its Substituted Analogues 2−4, and $\{[Me_2N(CH_2)_3]_2SnPh\}^+I^-$ (8). The solution stereochemistry of **1**, its aromatically substituted analogues **2**−**4**, and the triorganotin cation **8** was investigated at variable temperature by ^{1}H, ^{13}C, and ^{119}Sn NMR as well as by 1D ^{1}H−^{119}Sn HMQC spectroscopy (**1**−**4**).[1,4−8] Table 3 provides selected NMR data obtained at 303 and 223 K for **1**; the data for the compounds **2**−**4** are similar and are given in the Experimental Section. The ^{119}Sn NMR spectrum of **1** at 303 K displays a single resonance at −245.2 ppm ($W_{1/2}$ = 57 Hz). Upon temperature decrease, it becomes slightly sharper ($W_{1/2}$ = 45 Hz) and shifts to −256.9 ppm at 223 K, both values being close to the ^{119}Sn CP-MAS chemical shift of −250.7 ppm. The ^{1}H spectrum becomes increasingly complex as the temperature is lowered, all methylene protons become anisochronous, and the N−CH_3 resonance of **1** undergoes duplication below 248 K. Duplication of the *N*-methyl resonance is also observed in the ^{13}C NMR spectrum below 253 K, but no splitting of the signals of the methylene ^{13}C resonances occurs, indicating nonequivalence of protons within each methylene group but no loss of C_2 symmetry on the NMR time scale. At 223 K, the pairs of ^{1}H and ^{13}C resonances have sharpened. This spectral behavior is temperature reversible. The chemical shift difference of the ^{1}H and ^{13}C N−CH_3 resonances of **1** tends asymptotically to $\Delta\nu$ = 60 and 133 Hz, respectively. The aromatically substituted compounds **2**−**4** and the triorganotin cation **8** behave similarly, although in the latter case splitting of the ^{1}H and ^{13}C resonances is visible already at room temperature, and both the ^{119}Sn and ^{119}Sn CP-MAS resonances at −9.2 and −6.2 ppm, respectively, indicate pentacoordination at tin, in conformity with the solid-state structure. Furthermore, for each of the compounds **1**−**4** and **8** two equally intense N−CH_3 resonances are observed in the ^{13}C CP-MAS NMR spectra, in agreement with both skeleton chirality and its effective C_2 symmetry.

The free activation enthalpies of the dynamic processes as estimated from the temperature at which the CH_3N resonances coalesce in the ^{1}H and ^{13}C spectra amount respectively to $\Delta G^{\ddagger}_{248}$ = 49.0 kJ/mol and $\Delta G^{\ddagger}_{253}$ = 48.2 kJ/mol for **1**, $\Delta G^{\ddagger}_{243}$ = 47.9 kJ/mol and $\Delta G^{\ddagger}_{253}$ = 48.1 kJ/mol for **2**, $\Delta G^{\ddagger}_{263}$ = 52.6 kJ/mol and $\Delta G^{\ddagger}_{270}$ = 51.3 kJ/mol for **3**, $\Delta G^{\ddagger}_{240}$ = 47.0 kJ/mol and $\Delta G^{\ddagger}_{243}$ = 46.5 kJ/mol for **4**, and $\Delta G^{\ddagger}_{340}$ = 63.4 kJ/mol and $\Delta G^{\ddagger}_{328}$ = 64.1 kJ/mol for **8**. A value of the same order of magnitude was obtained for **1** in toluene-d_8 from the ^{1}H spectrum. Addition of water has negligible influence on the free activation enthalpies. Thus, $\Delta G^{\ddagger}_{243}$ = 47.8 kJ/mol and $\Delta G^{\ddagger}_{248}$ = 47.2 kJ/mol are estimated from the ^{1}H and ^{13}C NMR spectra of a sample of **1** in CD_2Cl_2

Table 2. Selected Bond Lengths (Å) and Angles (deg) for 1−4, 7, and 8[a]

	X = O				X = S	X = C
	1	**2**	**3**	**4**	**7**	**8**
Sn(1)−X(1)	2.063(2)	2.066(1)	2.100(2)	2.091(2)	2.501(1)	
Sn(1)−C(1)	2.118(3)	2.139(2)	2.130(2)	2.122(3)	2.131(3)	2.136(4)
Sn(1)−C(11)						2.137(4)
Sn(1)−C(21)						2.138(4)
Sn(1)−N(1)	2.646(3)	2.670(2)	2.575(2)	2.601(2)	2.908(3)	2.401(4)
Sn(1)−N(2)						2.392(4)
X(1)−Sn(1)−X(1A)	95.3(1)	94.15(8)	93.76(9)	93.5(1)	98.10(6)	
X(1)−Sn(1)−N(1A)	81.1(1)	80.94(6)	80.34(7)	171.56(8)	84.78(7)	
X(1)−Sn(1)−N(1)	170.1(1)	174.27(5)	171.45(7)	81.37(8)	171.94(7)	92.4(1)
X(1)−Sn(1)−N(2)						92.7(2)
X(1)−Sn(1)−C(1)	95.0(1)	101.74(7)	97.56(8)	98.64(9)	99.01(9)	
X(1)−Sn(1)−C(1A)	101.5(1)	96.13(7)	94.84(8)	96.34(9)	104.02(9)	
X(1)−Sn(1)−C(11)						113.1(2)
X(1)−Sn(1)−C(21)						115.2(2)
C(1)−Sn(1)−N(1)	76.8(1)	76.01(7)	76.93(8)	77.94(9)	73.0(1)	92.4(1)
C(1)−Sn(1)−N(1A)	88.0(1)	87.80 (7)	92.08(9)	88.63(9)	82.9(1)	
C(11)−Sn(1)−N(1)						81.1(2)
C(21)−Sn(1)−N(1)						95.3(2)
C(11)−Sn(1)−N(2)						98.5(2)
C(21)−Sn(1)−N(2)						81.0(2)
C(1)−Sn(1)−C(1A)	155.4(2)	153.7(1)	161.8 (1)	158.1(2)	144.6(2)	
C(11)−Sn(1)−C(21)						131.7(2)
N(1)−Sn(1)−N(1A)	103.9(2)	104.11(8)	106.2(1)	104.5(1)	93.4(1)	
N(1)−Sn(1)−N(2)						174.6(2)
C(11)−X(1)−Sn(1)	128.1(2)	125.8 (1)	130.9(1)	128.1(2)	102.6(1)	

[a] Symmetry transformations (A): 0.5 − *x*, 0.5 − *y*, *z* (**1**); −*x*, *y*, 0.5 − *z* (**2**); −*x*, −*y*, *z* (**3**); −*x* + 1, −*y*, *z* (**4**); −*x*, 0.5 − *y*, 0.5 − *z* (**7**).

Table 3. Selected ^{1}H, ^{13}C, and ^{117}Sn NMR Data for $[(Me_2N(CH_2)_3]_2Sn(EPh)_2$ (1, E = O; 7, E = S) and $[Me_2N(CH_2)_3]_2SnPh^+I^-$ (8)[a]

compd	nucleus	*T* (°C)	NCH_3	NCH_2	CH_2	$SnCH_2$	Sn
1	^{1}H[b]	+30	2.39 s	2.49 t	1.85 tt [160][c]	1.48 t [96][c]	
		−50	2.47/2.23	2.28/2.36	1.64/1.81 [*d*]	1.16/1.57 [*d*]	
	^{13}C[e]	+30	46.6	60.8 [56][f]	22.5 [38][f]	18.1 [832/795]	
		−50	47.7/45.6	60.3 [57][f]	22.4 [36][f]	16.8 [861/821]	
	^{119}Sn	+30					−245[g]
		−50					−257[g]
7	^{1}H	+30	1.99 s	1.95 t	1.49 tt [116][h]	1.20 t [70/65]	
		−50	1.92 s	1.79	2.47/2.23 [144][h]	0.98 [79][h]	
	^{13}C	+30	46.1	61.5 [57][i]	23.2 [33][i]	18.9 [520/497]	
		−50	46.9	60.7 [45][i]	23.1 [37][i]	19.7 [550][f]	
	^{117}Sn	+30					1.70 [493]
		−50					−45.3[j] [548]
8	^{1}H[k]	+30	2.34/1.77	2.59	2.06	1.80	
	^{13}C[l]	+30	47.0/46.2	61.4 [57]	21.8 [32]	9.8 [505]	
		+60	46.4	61.3 [58]	21.9 [31]	11.4	

[a] Chemical shifts δ (ppm) in CD_2Cl_2 (**1**), $C_6D_5CD_3$ (**7**), and $C_2D_2Cl_4$ (**8**); $J(^{119/117}Sn-^{1}H)$ and $J(^{119/117}Sn-^{13}C)$ couplings (in Hz) given in brackets. Abbreviations: (s) singlet, (t) triplet, (m) multiplet, (tt) triplet of triplets. [b] In $CDCl_3$ at +30 °C: o-Ph, 7.13, m; m-Ph, 6.93, m; p-Ph, 6.73, m. [c] Determined from a 1D gradient assisted $^{1}H-^{119}Sn$ HMQC NMR spectrum. [d] Immeasurable because of overlapping, broadness, and non-first-order effects. [e] In $CDCl_3$ at +30 °C: C_i, 161.3; C_o, 129.4; C_m, 119.2; C_p, 117.8. [f] Unresolved $^{n}J(^{13}C-^{119}Sn)$ and $^{n}J(^{13}C-^{117}Sn)$ coupling constants. [g] At a concentration of 43 mg of **1** per 0.5 mL of solvent. [h] Unresolved $^{2}J(^{1}H-^{119}Sn)$ and $^{2}J(^{1}H-^{117}Sn)$ coupling constants because of broadness and/or noise. [i] Estimated unresolved $^{n}J(^{13}C-^{119}Sn)$ and $^{n}J(^{13}C-^{117}Sn)$ coupling constants because of broadness and/or noise. [j] Minor signal (<2%) seen at −150.8 ppm. [k] Phenyl protons at 7.45. [l] C_i = 137.2; C_o = 135.0, $^{2}J(^{13}C-^{117/119}Sn)$ = 41; C_m = 129.7, $^{3}J(^{13}C-^{117/119}Sn)$ = 53; C_p = 129.9.

containing 1 molar equiv of D_2O. The ^{117}Sn spectrum at 303 K of **1** in the presence of 1 molar equiv of D_2O, however, reveals further broadening of the major ^{117}Sn resonance at −245 ppm ($W_{1/2}$ = 202 Hz) and the appearance of a very broad minor resonance (<10%) around −215 ppm ($W_{1/2}$ = 420 Hz). When the amount of D_2O is increased to 10 molar equiv (Figure 7), the relative amount of the minor species further increases to approximately 33% and both resonances broaden further (major, $W_{1/2}$ = 1070 Hz; minor, $W_{1/2}$ = 1300 Hz), indicating mutual exchange. However, the most remarkable observation is that, at 223 K, in the ^{117}Sn spectra of all samples of **1**, whether moisture free or with 1 or 10 molar equiv of D_2O, the signal for the minor species completely disappears and a single narrow resonance at −257 ppm ($W_{1/2}$ = 43 Hz) is observed, with a $^{1}J(^{13}C-^{119/117}Sn)$ coupling constant of ca. 860/830 Hz. These observations are temperature reversible.

There is no noticeable concentration effect on the ^{119}Sn chemical shifts and the $^{1}J(^{13}C-^{119/117}Sn)$ coupling constants, at either 303 or 223 K. This excludes that oligomerization is responsible for the above low-frequency shift of the ^{119}Sn resonance and $^{1}J(^{13}C-^{119/117}Sn)$ coupling increase upon temperature decrease.

In addition to the coalescence phenomena observed for the ^{1}H and ^{13}C N−CH_3 resonances the $^{2}J(^{13}C-O-^{119/117}Sn)$ couplings are also temperature dependent. Thus, at 223 K, both **1** and **2** exhibit $^{2}J(^{13}C-O-^{119/117}Sn)$ satellites of 33 Hz at the C_{ipso} resonance of the phenolate or *p-tert*-butyl-substituted phenolate ligand, which dis-

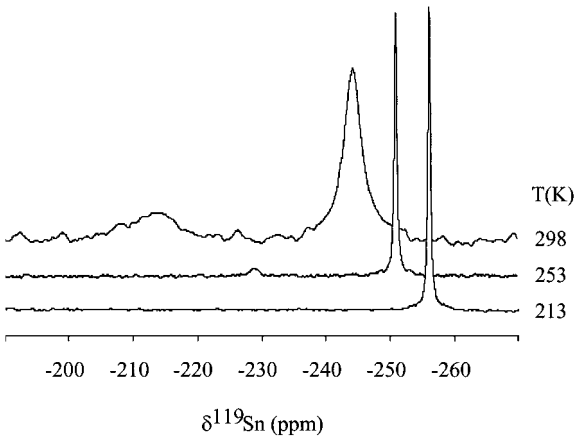

Figure 7. ^{119}Sn NMR(CD_2Cl_2) spectrum of compound **1** in the presence of 10 molar equiv of H_2O at three different temperatures.

appear at room temperature, indicating Sn−O bond rupture. These satellite coalescences take place in the same temperature range as the N−Me resonance coalescence, as supported by estimated activation free enthalpies of $\Delta G^{\ddagger}_{250} = 50.5$ kJ/mol and $\Delta G^{\ddagger}_{244} = 49.2$ kJ/mol for **1** and **2,** respectively, of the same order as those found from the coalescences of the N−Me resonances. Significantly, mixing **1** and **2** in the molar ratio 1:1 provided a single broad ^{117}Sn resonance at room temperature and three sharp resonances in the approximate ratio 1:2:1 at 223 K, which indicates a scrambling reaction with Sn−O bond cleavage to give the mixed species $[Me_2N(CH_2)_3]_2Sn(OC_6H_5)(OC_6H_4$-*t*-Bu-4). Also at 223 K, the 1D ^{1}H−^{119}Sn HMQC spectrum[1,4−8] of **1** exhibits strong ^{1}H−^{119}Sn correlations of the ^{119}Sn resonance with one of the two methyl resonances of the NMe_2 moiety. Strong correlations with the *ortho* proton resonances and even weaker correlations with the *meta*/*para* protons of the phenolate moiety are likewise observed. This indicates the existence of a bond between the tin atom and the phenolate oxygen with a lifetime of at least the ^{1}H−^{119}Sn HMQC evolution time (≫90 ms).[4c] In contrast, at room temperature, none of the ^{1}H−^{119}Sn HMQC correlations of the ^{119}Sn nucleus with the phenolate protons remain visible, while correlations with all the averaged aliphatic proton resonances are observed, including with the exchange-averaged N−Me resonance. This confirms that at room temperature the Sn−OPh bond is lost on the ^{1}H−^{119}Sn HMQC NMR time scale as well. A similar observation was already made for the Sn−F bond of $[Me_2N(CH_2)_3]_2SnF_2$,[4c] which appeared to be kinetically more labile than the N→Sn bond.

The *o*-fluorophenolate analogue **4** behaves similarly. Despite limited solubility hampering detailed coupling satellite analysis in the ^{13}C spectra, a ^{19}F−^{117}Sn HMQC experiment[4c] exhibited a $^4J(^{19}F-C-C-O-^{117}Sn)$ correlation at 223 K, but none at room temperature, in complete agreement with the behavior of **1** and **2**. The *p*-nitrophenolate derivative **3** exhibits too low a solubility for a detailed coupling satellite analysis.

One possibility to explain the temperature-dependent NMR spectroscopic results is the following. At low temperature, the compounds **1**−**4** are rigid on the ^{1}H and ^{13}C NMR time scales, with the N−CH_3 groups being diastereotopic, as supported by the anisochrony of their

Scheme 1

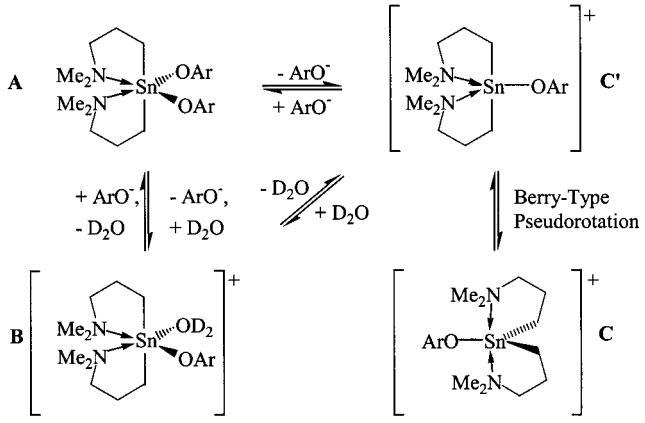

resonances. This feature, combined with the absence of any splitting of their single ^{119}Sn resonance upon temperature decrease indicates the presence of only one single chiral diastereomer. These low-temperature data are therefore consistent with **1**−**4** having similar *cis* structures for the phenolate moieties in solution as well as in the solid state and existing consequently as a pair of enantiomers. The same observation holds for compound **8**, which at low temperature exists as a pair of enantiomers with pentacoordinated tin. Two processes are proposed to account for the coalescence phenomena observed in the ^{1}H and ^{13}C NMR spectra. The first one is insufficient and even not necessarily rate-determining for the enantiomerization and is shown in Scheme 1. It involves Sn−OAr bond cleavage in the complex **A** and formation of the pentacoordinated cation **C** or, in the presence of water, the hexacoordinated cationic aqua adduct **B**. The population of species **C** is low, as supported by the averaged ^{119}Sn chemical shift being indicative of six- rather than five-coordination at tin. The formation of **C** necessarily passes through the highly energetic pentacoordinated transition state or intermediate **C′** with two axial carbons violating the polarity rule[15] but which is directly converted into **C** by a one-step Berry pseudorotation.[16] This effectively (i) brings the two NMe_2 groups into the favored axial positions of the trigonal bipyramid, as expected on the basis of the polarity rule,[15] and (ii) allows the five-membered chelate rings to adopt the least strained axial−equatorial arrangement. Essential to note at this stage is that the set of processes of Scheme 1 cannot lead on its own to enantiomerization of the propeller skeleton of the original hexacoordinated complex **A**. According to the principle of microreversibility,[17,18] half of an enantiomerization pathway from the initial state to the transition state has to be the mirror image of the other half of the pathway from the transition state to the final mirror image state, and vice versa. This necessarily results in the transition state being achiral.[19−23] Hence, in order for **A** to enantiomerize, **C**

(15) Bent, H. A. *Chem. Rev.* **1961**, *61*, 275.
(16) Berry, R. S. *J. Chem. Phys.* **1960**, *32*, 933.
(17) De Groot, S. R.; Mazur, P. *Non Equilibrium Thermodynamics*; North-Holland: Amsterdam, 1962.
(18) Burwell, R. G.; Pearson, R. G. *J. Phys. Chem.* **1966**, *70*, 300.
(19) Stanton, R. E.; McIver, J. W. *J. Am. Chem. Soc.* **1975**, *97*, 3632.
(20) Pechukas, P. *J. Chem. Phys.* **1976**, *64*, 1516.
(21) Nourse, J. G. *J. Am. Chem. Soc.* **1980**, *102*, 4883.
(22) Willem, R. *Prog. NMR Spectrosc.* **1987**, *20*, 1.
(23) Brocas, J.; Willem, R. *J. Am. Chem. Soc.* **1983**, *105*, 2217.

Scheme 2

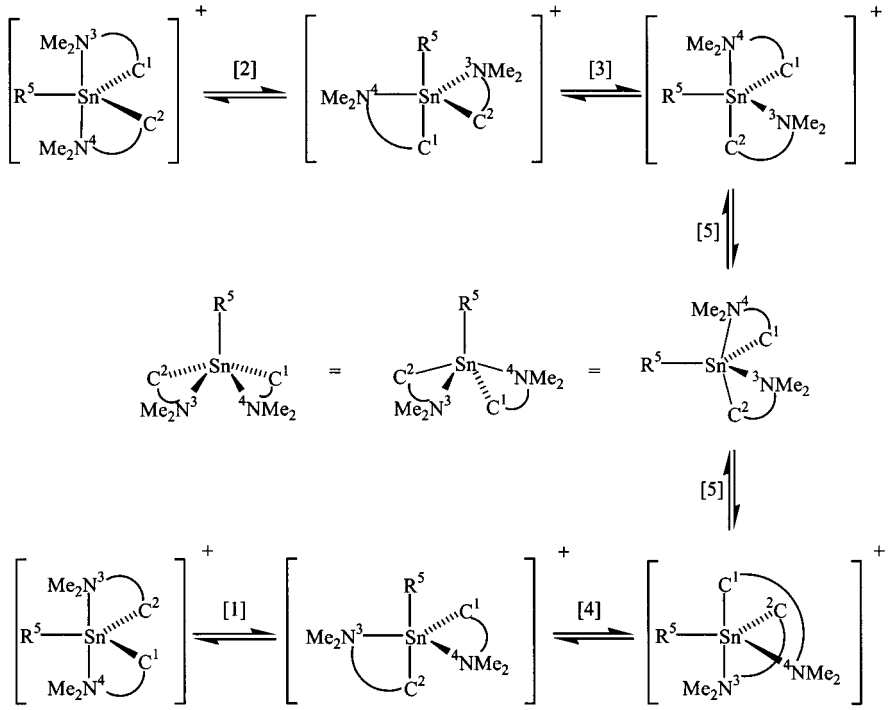

has to enantiomerize, which can be achieved either by a 2-fold Sn−N dissociation passing through achiral three- or four-coordinate intermediates/transition states or by a sequence of five steps of Berry-type pseudorotations (Scheme 2) containing itself an achiral square-pyramidal transition.[16] Each of the five Berry pseudorotations has to occur each time with a different pivot,[24] so that all pivots are involved at least but also only once.[25] The latter proposal considers as unrealistic any alternative regular process involving directly square-pyramidal five-coordinate structures as intermediates rather than trigonal-bipyramidal ones. In any event, using a sequence of Berry pseudorotations implies involvement of square pyramids, since these are transition states or intermediates for the Berry pseudorotation of the trigonal bipyramids.[16,25] Although the experimental data at hand do not allow *unambiguous* discrimination between these two pathways, the very similar free activation enthalpies estimated for phenolate derivatives **1**−**4** as well as the much higher free activation enthalpy observed for the triorganotin cation **8**, corresponding to a trigonal-bipyramidal structure in which the electronegative arylolate has been replaced by a more electropositive phenyl ligand, suggest the chain of Berry-type pseudorotations to be operative. Thus, in this view, the high free activation enthalpy for the enantiomerization of **8** is a result of passing through energetically very unfavored trigonal-bipyramidal structures with two carbon atoms in axial positions (second and fifth trigonal-bipyramidal structures in Scheme 2, against the polarity rule[15]), which does not hold for compounds **1**−**4**, where only one carbon at a time is in an axial position. The same sequence of Berry pseudorotations was invoked by Martin et al. to explain the inversion of configuration of related siliconate derivatives.[26a] Notably, in dichloromethane solution compound **8** is a contact ion pair (molar conductivity $l = 2.55$ S cm^2 mol^{-1}) whereas in acetonitrile it exists as an independent cation and anion ($l = 12.34$ S cm^2 mol^{-1}). Nevertheless, the free activation enthalpy of $\Delta G^{\ddagger}_{348} = 68$ kJ/mol for the dynamic process, as estimated from the temperature at which the CH_3N resonances coalesce in the ^{1}H spectrum in acetonitrile, is very close to the corresponding value in dichloromethane and indicates the effect of solvents on the proposed mechanism to be negligible.

Our interpretation gets further support from a comparison with the intramolecularly coordinated bis(2-((dimethylamino)methyl)ferrocenyl)tin dichloride (2-$Me_2NCH_2C_5H_3FeCp)_2SnCl_2$,[26b] the intramolecular Sn−N distances (2.888(10)/2.885(10) Å) in the solid state of which are much longer than those in compounds **1**−**4**. However, its enantiomerization proceeds with a free activation enthalpy of $\Delta G^{\ddagger}_{232} = 47.2$ kJ/mol, which is in the range of the corresponding values estimated for the phenolate derivatives **1**−**4**. It seems to be likely that, in analogy to the mechanism proposed to account for the dynamic behavior of compounds **1**−**4**, the enantiomerization of (2-$Me_2NCH_2C_5H_3FeCp)_2SnCl_2$ proceeds via Sn−Cl bond dissociation and formation of the pentacoordinated cation [(2-$Me_2NCH_2C_5H_3FeCp)_2SnCl]^+$ followed by a five-step Berry pseudorotation rather than by a 2-fold Sn−N dissociation.

Solution Stereochemistry of $[Me_2N(CH_2)_3]_2Sn(SPh)_2$ (7). The solution stereochemistry of the dithiophenolate **7** in $C_6D_5CD_3$ was investigated at 303 and 223 K by ^{1}H, ^{13}C, and ^{117}Sn NMR as well as by 1D ^{1}H−

(24) The pivot is the ligand of the five-coordinate trigonal bipyramid which remains immobile, i.e., at the equatorial position, during a Berry pseudorotation.[23,25]

(25) Brocas, J.; Gielen, M.; Willem, R. *The Permutational Approach to Dynamic Stereochemistry*; McGraw-Hill: New York, 1983; Chapter 14.

(26) (a) Stevenson, W. H., III; Wilson, S.; Martin, J. C.; Farnham, W. B. *J. Am. Chem. Soc.* **1985**, *107*, 6340. (b) Krüger, C.; Thiele, K.-H.; Meunier-Piret, J.; Dargatz, M.; Jurkschat, K. Unpublished results.

Scheme 3

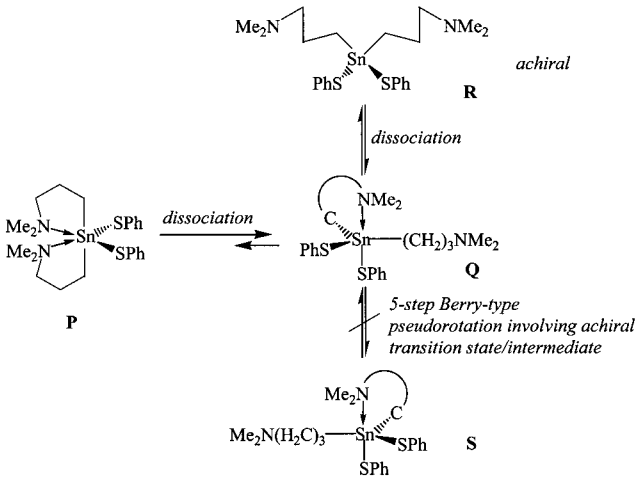

^{117}Sn HMQC spectroscopy (Table 3). The ^{117}Sn NMR data are essentially concentration independent, indicating no intermolecular interaction. Only a single, narrow ^{117}Sn resonance is observed at all temperatures and concentrations, up to a minor narrow resonance around −150 ppm (<2%) in the concentrated sample at low temperature, which appears insignificant and was not assigned. The major ^{117}Sn resonance is temperature dependent and shifts from 1.7 ppm at 303 K to −45.3 ppm at 223 K, with the latter value being close to the ^{119}Sn CP-MAS chemical shift of −37.5 ppm. Associated with the low-frequency ^{117}Sn chemical shift upon temperature decrease is an increase of the $^{1}J(^{117}\mathrm{Sn}-^{13}\mathrm{C})$ coupling from 493 to 548 Hz. On the other hand, both the ^{1}H and ^{13}C NMR spectra do not show, except slight changes in chemical shifts, any decoalescence or even broadening of the methyl and methylene signals on going from 303 to 223 K, a behavior similar to that reported for $\{[Me_2N(CH_2)_3]_2SnS\}_2$.[12] These results can be interpreted in terms of compound **7** being involved in equilibria between species **P**, **Q**, and **R** (Scheme 3). These equilibria are fast on the ^{1}H, ^{13}C, and ^{119}Sn NMR time scales even at low temperature. The population of the tetracoordinated species **R** in the equilibria is neglibly low, as the ^{119}Sn chemical shift would be expected at about 120 ppm, on the basis of comparison with tetracoordinated $Me_2Sn(SPh)_2$ ($\delta(^{119}\mathrm{Sn})$ 122.5 ppm).[27a] At room temperature the pentacoordinated species **Q** dominates, whereas at low temperature the population of **P** ("4 + 2"-coordinate) is increased, as is supported by the similarity of the $\delta(^{119}\mathrm{Sn})$ value in solution and the isotropic $\delta(^{119}\mathrm{Sn})$ value in the CP-MAS spectrum.

The obvious "4 + 2"- rather than 6-coordination nature of the organotin thiophenolate derivative **7**, evidenced by its much longer Sn−N bonds as compared to the organotin phenolate derivatives **1**−**4**, supports Scheme 3. Its essential basis is the easy Sn−N dissociation from "4 + 2"-coordinate **P** to 5-coordinate **Q**, and, subsequently, to 4-coordinate achiral **R**. The absence of any observable decoalescence of the N−Me resonances upon temperature lowering, unlike **1**−**4**, also supports

(27) (a) Kennedy, J. D.; McFarlane, W. *J. Chem. Soc., Perkin Trans. 2* **1974**, 146. (b) Kumar Das, V. C.; Keong, Y. C.; Wie, C.; Smith, P. J.; Mak, T. C. W. *J. Chem. Soc., Dalton Trans.* **1987**, 129. (c) Kost, D.; Kalikhman, I.; Raban, M. J. *J. Am. Chem. Soc.* **1995**, *117*, 11512.

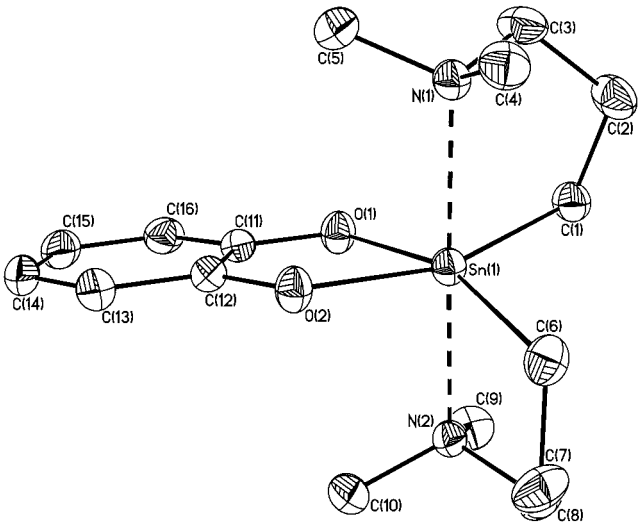

Figure 8. General view (SHELXTL) of a molecule showing 30% probability displacement ellipsoids and the atom numbering for **5**.

the proposal of occurrence of a different mechanism, the two Sn−N bonds being obviously very weak for **7**, which henceforth remains achiral on the NMR measuring time scale, indicating a very low activation barrier for enantiomerization. While it cannot formally be excluded that a sequence of five Berry steps invoked for **1**−**4** would also occur for **7** from **Q** to **S** (Scheme 3), the latter looks unlikely because there is no apparent reason such a sequence would occur with a lower activation barrier for the conversion from **Q** to **S** in **7** than for the sequence of Scheme 2 for **1**−**4**. In contrast, an analysis similar to Scheme 2 of the five-Berry-step sequence for the conversion from **Q** to **S** reveals that the sequence would require (i) a trigonal bipyramid (TBP) with two apical carbons, in strong violation of the polarity rule, (ii) a TBP with one apical carbon and the bidentate C−N ligand spanning a diequatorial configuration, in violation of both the polarity rule *and* the geometrical ligand constraint, or (iii) a TBP spanning the diapical configuration, in violation of the geometrical ligand constraint. These three configurations are obviously sufficiently energetically unfavorable to make fast enantiomerization of **7**, as observed, through the conversion from **Q** to **S** by five Berry pseudorotation steps highly unlikely.

Unlike the diphenolate derivatives **1**−**4** and the triorganotin iodide derivative **8**, the nonequivalence of the N−CH_3 carbons in **7** as established by X-ray analysis is not reflected by its ^{13}C CP-MAS spectrum. The single NCH_3 isotropic shift observed at 49.5 ppm is ascribed to accidental isochrony.

The ^{1}H−^{117}Sn HMQC spectra display deceptively uninformative patterns, since a ^{1}H−^{117}Sn correlation is observed between all ^{1}H resonances and the single ^{117}Sn resonance at both temperatures, including all aromatic thiophenolate ^{1}H signals. This supports the equilibria as proposed in Scheme 3 and shows that no intermolecular exchange of PhS^- ligands is occurring on a measurable NMR time scale.

Molecular Structures of the Stannaindane Derivatives 5 and 6. The molecular structures of compounds **5** and **6** are shown in Figures 8 and 9, respectively. The crystallographic data are given in Table 1 and selected bond lengths and bond angles are sum-

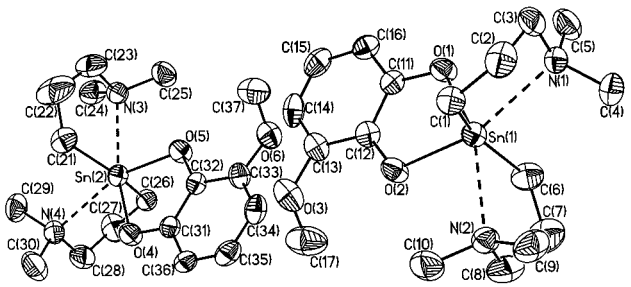

Figure 9. General view (SHELXTL) of molecules showing 30% probability displacement ellipsoids and the atom numbering for **6a** and **6b**.

marized in Table 4. In contrast to the tin atoms in the diorganotin diphenolate derivatives **1**−**4**, the metal center in the stannaindane derivative **5** exhibits a distorted-octahedral configuration with both the carbon and oxygen atoms *cis* and the nitrogen atoms mutually *trans*.

The distortion from the ideal octahedral configuration is manifested in the deviation of the N(1)−Sn(1)−N(2), O(1)−Sn(1)−C(6), and O(2)−Sn(1)−C(1) angles of 177.9(6), 161.2(8), and 162.5(1)°, respectively, from the ideal value of 180°. The Sn(1)−N(1) and Sn(1)−N(2) distances of 2.362(2) and 2.377(2) Å, respectively, are rather short and compare well with the corresponding distances in $[Me_2N(CH_2)_3]_2SnF_2 \cdot 2H_2O$.[4c] Unlike the case of the triorganotin cation **8**, the nonequivalence of all carbon atoms of compound **5** in the solid is only partially reflected by its ^{13}C CP-MAS NMR spectrum showing four out of six resonances for the aromatic carbons, five out of six resonances for the methylene carbons, and two out of four resonances for the methyl carbons.

The methoxy-substituted stannaindane derivative **6** crystallizes as a 1:1 mixture of the two diastereomers **6a** and **6b**, which are both chiral and hence exist as pairs of enantiomers.

The existence of the two diastereomers is also reflected by the observation of two equally intense ^{119}Sn CP-MAS resonances at −193.0 and −199.8 ppm. As in the related derivative **5**, the tin atoms in **6a** and **6b** show a distorted-octahedral configuration but with the somewhat surprising difference that, as for the phenolate derivatives **1**−**4**, (i) the two carbon atoms in each diastereomer are again mutually *trans* with C−Sn−C angles of 154.4(2) and 154.1(3)°, respectively, whereas the two nitrogen and two oxygen atoms are *cis*, and (ii) the Sn−N distances of 2.529(5)−2.594(5) Å are longer than those in compound **5**. The latter result is in line with the observation made by Kumar Das et al. that octahedral *cis*- and *trans*-SnR_2 isomeric adducts of dichlorobis(4-chlorophenyl)tin(IV) with 4,4′-dimethyl-2,2′-bipyridyl exhibit rather different Sn−N distances.[27b]

Solution Stereochemistry of the Stannaindane Derivatives 5 and 6. The ^1H, ^{13}C, and $^{117/119}Sn$ NMR spectral behavior of compounds **5** and **6** at low and room temperature is similar to that of compounds **1**−**4**, up to one essential point.

Indeed, $^3J(^{13}C-C-O-^{119}Sn)$ couplings, as well as $^1H-^{119}Sn$ HMQC correlations between aromatic protons and the ^{119}Sn nucleus, are now observed at both room and low temperature and even at high temperature in toluene (353 K). This holds also for the methoxy proton resonance of **6**. This means that, in contrast to the

Scheme 4

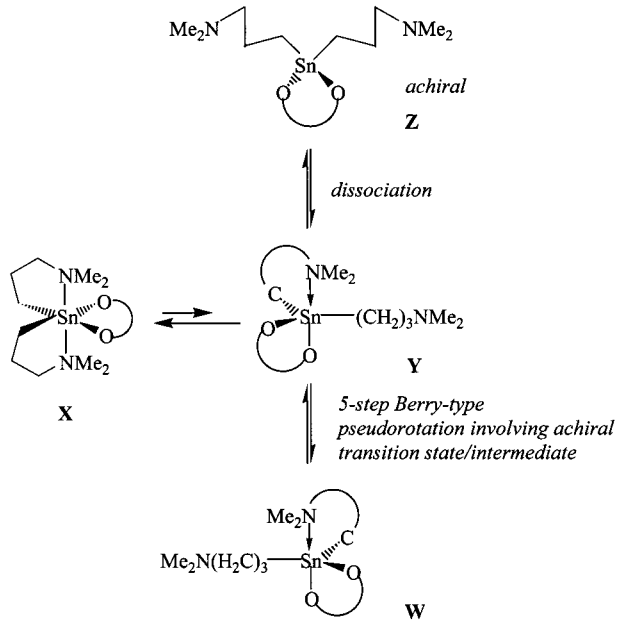

phenolate derivatives **1**−**4**, the catecholate dianion or its methoxy-substituted analogue is not released into the medium upon enantiomerization of **5** and **6**. In the specific case of **6**, the three N−Me resonances observed in the intensity ratio 2:1:1 in the ^1H and ^{13}C NMR spectra at low temperature coalesce to a single resonance at room temperature, reflecting that the enantiomerization is indeed accompanied by mutual exchange of the chemical environments of the two $Me_2N(CH_2)_3-$ chains. It cannot be determined whether a single coalescence, rather than a stepwise coalescence, as proposed by Kost et al. for six-coordinate silicon complexes,[27c] occurs for the N−Me resonances, because the two rate processes tend to overlap, a complex coalescence pattern being observed over a wide range of temperature, rather than two well-separated ones in two temperature ranges. Moreover, in the case of the proton spectra, a coalescence analysis is impossible, because the coalescing N−Me proton resonances overlap with the complex, non-first-order resonances of the methylene protons, which themselves all undergo unanalyzable coalescence phenomena. For this reason a reliable estimation of such free activation enthalpies was not achieved for the methoxy-substituted stannaindane derivative **6**. The ^{117}Sn NMR spectrum of **6** in CD_2Cl_2 (303 K, $\delta(^{117}Sn)$ −181.2, $W_{1/2}$ = 46 Hz; 223 K, $\delta(^{117}Sn)$ −191.1, $W_{1/2}$ = 50 Hz) is almost temperature independent and does not, even at low temperature, split into two resonances, despite the two diastereomeric pairs of enantiomers that might a priori be expected from the presence of two such species in the solid state. This result indicates that the two diastereomeric species merge into one single diastereomer upon dissolution.

A mechanism which accounts for the enantiomerization and which is compatible with the NMR data at hand as well as with the principle of microreversibility is proposed in Scheme 4. The hexacoordinated species **X** undergoes intramolecular Sn−N dissociation and is in a non-rate-determining equilibrium with the pentacoordinated species **Y**. This process, however, is not sufficient to achieve enantiomerization, as no interme-

Table 4. Selected Bond Lengths (Å) and Angles (deg) for 5, 6a, and 6b

	5	6a		6b
Sn(1)−O(1)	2.107(1)	2.073(2)	Sn(2)−O(4)	2.084(2)
Sn(1)−O(2)	2.104(1)	2.090(2)	Sn(2)−O(5)	2.075(2)
Sn(1)−C(1)	2.174(2)	2.128(3)	Sn(2)−C(21)	2.125(3)
Sn(1)−C(6)	2.179(2)	2.129(3)	Sn(2)−C(26)	2.132(3)
Sn(1)−N(1)	2.362(2)	2.524(3)	Sn(2)−N(3)	2.548(3)
Sn(1)−N(2)	2.377(2)	2.572(3)	Sn(2)−N(4)	2.587(3)
O(1)−Sn(1)−O(2)	77.75(6)	80.12(9)	O(4)−Sn(2)−O(5)	80.77(9)
O(1)−Sn(1)−N(2)	85.75(7)	158.9(1)	O(4)−Sn(2)−N(4)	80.5(1)
O(1)−Sn(1)−N(1)	93.76(7)	82.43(9)	O(4)−Sn(2)−N(3)	161.5(1)
O(1)−Sn(1)−C(1)	90.32(9)	101.6(1)	O(4)−Sn(2)−C(21)	97.6(1)
C(1)−Sn(1)−N(1)	80.81(8)	77.8(1)	C(21)−Sn(2)−N(3)	77.3(1)
C(1)−Sn(1)−N(2)	97.17(8)	89.2(1)	C(21)−Sn(2)−N(4)	89.0(1)
C(1)−Sn(1)−C(6)	103.8(1)	154.3(1)	C(21)−Sn(2)−C(26)	154.4(2)
O(2)−Sn(1)−C(1)	162.53(9)	99.9(1)	O(5)−Sn(2)−C(26)	100.8(1)
O(2)−Sn(1)−C(6)	90.79(9)	99.0(1)	O(5)−Sn(2)−C(26)	99.4(1)
O(2)−Sn(1)−N(2)	94.65(7)	80.1(1)	O(5)−Sn(2)−N(4)	159.8(1)
O(2)−Sn(1)−N(1)	87.21(7)	161.56(9)	O(5)−Sn(2)−N(3)	82.7(1)
C(6)−Sn(1)−N(1)	100.64(9)	89.5(1)	C(26)−Sn(2)−N(3)	89.9(1)
C(6)−Sn(1)−N(2)	80.28(8)	77.0(1)	C(26)−Sn(2)−N(4)	77.0(1)
N(1)−Sn(1)−N(2)	177.92(6)	117.9(1)	N(3)−Sn(2)−N(4)	116.9(1)
O(1)−Sn(1)−C(6)	161.17(8)	98.7(1)	O(4)−Sn(2)−C(26)	101.0(1)
C(11)−O(1)−Sn(1)	113.6(2)	112.4(2)	C(31)−O(4)−Sn(2)	111.4(4)
C(12)−O(2)−Sn(1)	114.2(1)	111.0(2)	C(32)−O(5)−Sn(2)	110.2(2)

diate/transition state with achiral molecular skeleton is involved. To achieve enantiomerization, species **Y** can undergo either a second intramolecular Sn−N bond dissociation involving the achiral tetracoordinated species **Z** or a five-step sequence of Berry-type pseudorotations to generate the enantiomer of species **Y**: i.e., species **W**. With the data at hand these two mechanisms cannot be distinguished unambiguously. However, on the basis of the free activation enthalpies of $\Delta G^{\ddagger}_{258} =$ 50.5 kJ/mol and $\Delta G^{\ddagger}_{263} =$ 49.2 kJ/mol, as estimated from the temperature at which the NCH_3 resonances coalesce in the ^{1}H and ^{13}C spectra of compound **5** and which are very similar to the values for compounds **1**−**4**, we suggest the Berry pseudorotation to be operative.

Conclusion

The results presented here demonstrate that isomerizations of hypercoordinated organotin compounds containing two intramolecularly coordinating built-in ligands such as the (dimethylamino)propyl group and at least one electronegative substituent X such as phenolate or thiophenolate may proceed either via rupture of the intramolecular coordination or via ionic pentacoordinated intermediates generated by heterolytic Sn−X bond dissociation. Both mechanisms can proceed independently from one another. Nevertheless, facile enantiomerization processes through Berry pseudorotations in the pentacoordinated intermediates cannot proceed without preliminary Sn−X bond rupture, while the latter bond rupture is not a sufficient condition for enantiomerization of the orginal hexacoordinated complexes.

The different behaviors observed for the diorganotin diphenolate derivatives **1**−**4** and the diorganotin dithiophenolate **7** can be traced to the higher ionic character of the Sn−O versus the Sn−S, bond which makes the former kinetically more labile. The methodology reported here may also apply to the investigation of enantiomerizations and epimerizations of chiral hypercoordinated organotin compounds, which have received increasing attention as reagents in organic synthesis.

Experimental Section

NMR Experiments. The ^{1}H, ^{13}C, and ^{119}Sn (or ^{117}Sn) NMR spectra were recorded at 303 K in $CDCl_3$ or in CD_2Cl_2, on Bruker AMX500, DRX 400, DPX300, and DRX250 spectrometers. The ^{19}F NMR spectrum was recorded at 303 K in CD_2Cl_2, on the Bruker DRX250 spectrometer tuned to 235.35 MHz. ^{1}H and ^{13}C chemical shifts were referenced to the residual solvent peak and converted to the standard Me_4Si scale by adding 7.23 and 77.0 ppm ($CDCl_3$) or 5.32 and 53.8 (CD_2Cl_2) for ^{1}H and ^{13}C nuclei, respectively. For ^{119}Sn and ^{117}Sn chemical shifts, $\Xi =$ 37.290 665 and 35.632 295 MHz[28,29] were respectively used. For the ^{19}F chemical shift of compound **4**, $\Xi =$ 94.094 003 MHz[29] was used. ^{13}C and ^{119}Sn MAS spectra were obtained from a Bruker MSL 400 spectrometer using cross-polarization and high-power proton decoupling.

Chemical shift data are provided in ppm, with coupling constants in Hz. Abbreviations used are as follows: s = singlet; d = doublet; dd = doublet of doublets; t = triplet; tt = triplet of triplets; m = complex multiplet.

The gradient pulsed proton detected 1D ^{1}H−^{119}Sn HMQC correlation spectra were acquired as illustrated recently.[4c,5c,g,30−33] Typical evolution times, as used for compound **1**, were 23, 50, 60, and 90 ms at 213 K, and 23, 40, 50, 120, and 280 ms at 303 K. The ^{117}Sn nucleus was chosen for the tin and proton tin HMQC NMR spectra recorded on the DRX 250 spectrometer for reasons of local radio interference giving rise to poorer signal-to-noise ratio with the ^{119}Sn nucleus.

The electron ionization mass spectra were recorded on a Finnigan MAT 8230 spectrometer.

The conductivity measurements were performed at 20 °C in CH_2Cl_2 and CH_3CN, respectively, on a conductivity measuring device LF 530 of the WTW company, equipped with a Phillips cell of cell constant $k = 0.79$ cm^{-1}.

(28) Davies, A. G.; Harrison, P. G.; Kennedy, J. D.; Puddephatt, R. J.; Mitchell, T. N.; McFarlane, W. *J. Chem. Soc. A* **1969**, 1136.
(29) Mason, J. *Multinuclear NMR*; Plenum Press: New York, 1987; p 627.
(30) Willem, R.; Bouhdid, A.; Kayser, F.; Delmotte, A.; Gielen, M.; Martins, J. C.; Biesemans, M.; Tiekink, E. R. T. *Organometallics* **1996**, *15*, 1920.
(31) Kayser, F.; Biesemans, M.; Gielen, M.; Willem, R. *J. Magn. Reson. A* **1993**, *102*, 249.
(32) Kayser, F.; Biesemans, M.; Gielen, M.; Willem, R. In *Physical Organometallic Chemistry, Advanced Applications of NMR to Organometallic Chemistry*; Gielen, M., Willem, R., Wrackmeyer, B., Eds.; Wiley: Chichester, U.K., 1996; Chapter 3, p 45.
(33) Martins, J. C.; Verheyden, P.; Kayser, F.; Gielen, M.; Willem, R.; Biesemans, M. *J. Magn. Reson.* **1997**, *124*, 218.

Crystallography. Intensity data for the colorless (**1**−**4**, **7**, **8**) and violet (**5**, **6**) crystals were collected on Nonius MACH3 (**7**) and KappaCCD (**1**−**6**, **8**) diffractometers with graphite-monochromated Mo Kα radiation (0.710 69 Å) at 291 K. Three standard reflections were recorded every 60 min (**7**), and an anisotropic intensity loss up to 1.1% was detected during X-ray exposure. The data collection for **1**−**6** and **8** covered the whole sphere of reciprocal space with 360 frames via ω-rotation ($\Delta/\omega = 1°$) at 2 times 2 s (**1**), 5 s (**4**) 10 s (**2**, **3**, **6**), 20 s (**4**, **8**), and 60 s (**5**) per frame. The crystal to detector distance was 2.6 cm (**1**), 2.8 cm (**8**), and 3.0 (**2**−**6**) cm with a detector θ offset of 5° (**2**−**6**). Crystal decay was monitored by repeating the initial frames at the end of data collection. When the duplicate reflections were analyzed, there was no indication for any decay (**1**−**4**, **7**, **8**). The structures were solved by direct methods (SHELXS97)[34a] and successive difference Fourier syntheses. Refinement applied full-matrix least-squares methods (SHELXL97).[34b]

The H atoms were placed in geometrically calculated positions using a riding model and refined with common isotropic temperature factors for different C−H types (C_{prim}−H = 0.96 Å, C_{sec}−H = 0.97 Å, U_{iso} = 0.080(4) (**1**), 0.100(2) (**2**), 0.091(3) (**3**), 0.077(3) (**4**), 0.064(2) (**5**), 0.114(2) (**6**), 0.099(7) (**7**), 0.094(4) (**8**) Å^2; C_{aryl}−H = 0.93 Å, U_{iso} = 0.075(6) (**1**), 0.045(3) (**2**), 0.059(4) (**3**), 0.062(5) (**4**), 0.060(4) (**5**), 0.062(4) (**6**), 0.105-(5) (**7**), 0.076(7) (**8**) Å^2).

A disordered (dimethylamino)propyl group was found in **7** with occupancies of 0.60 (C(2), C(3), C(5)) and 0.40 (C(2′), C(3′), C(5′)),

The absolute configurations for **1**, **3**, **4**, and **8** could not be determined by refinement of the Flack[34c] parameter. The correctness of the absolute configurations was deduced from the X-ray data by comparison of the *R* values of inverted and noninverted structures.

Atomic scattering factors for neutral atoms and real and imaginary dispersion terms were taken from ref 34d. Figures were created by SHELXTL.[34e] Crystallographic data are given in Table 1, and selected bond distances and bond angles are listed in Tables 2 (**1**−**4**, **7**, **8**) and 3 (**5**, **6**).

Synthesis of the Bis(3-(dimethylamino)propyl)tin Diphenolate Derivatives 1−4. A solution of bis(3-(dimethylamino)propyl)diphenyltin (1.50 g, 3.37 mmol) and an excess of the corresponding phenol (13.49 mmol) in toluene was heated at reflux for 6.5 h. The toluene, the excess phenol, and the benzene formed during the reaction were removed under reduced pressure to give a residue which was recrystallized from the appropriate solvent.

1: 1.27 g of phenol; yield 0.76 g (47%); colorless crystals (from toluene); mp 179 °C. ^{1}H NMR (400.13 MHz, $CDCl_3$): 1.52 (t, 4H, $SnCH_2$), 1.83 (m, 4H, CCH_2), 2.40 (s, 12H, NCH_3), NCH_2 is partially overlapping with NCH_3; 6.73 (m, 2H, p-Ph), 6.93 (m, 4H, m-Ph), 7.13 (m, 4H, o-Ph). ^{13}C NMR (100.63 MHz, $CDCl_3$): 7.4 ($^1J(^{119/117}Sn-^{13}C)$ = 829/788 Hz, $SnCH_2$), 21.9 ($^2J(^{119/117}Sn-^{13}C)$ = 38 Hz, CCH_2), 46.3 (NCH_3); 60.7 ($^3J(^{119/117}Sn-^{13}C)$ = 56 Hz, NCH_2); 161.4 (C_i); 129.4 (C_o); 119.2 (C_m); 117.8 (C_p). ^{13}C CP-MAS NMR (100.63 MHz): 164.5, 130.5, 129.2, 120.2, 118.3 (phenyl carbons), 59.7 (NCH_2), 47.9 (NCH_3), 43.2 (NCH_3), 28.7 (CH_2), 14.9 ($SnCH_2$). ^{119}Sn NMR (186.50 MHz, CD_2Cl_2): −239.3. ^{119}Sn CP-MAS NMR (149.21 MHz): −250.7. Mass spectrum: *m/e* 385 ($C_{16}H_{29}N_2OSn^+$), 292 ($C_{10}H_{24}N_2OSn^+$), 206 ($C_5H_{12}NSn^+$). Anal. Found: C, 55.3; H, 7.3; N, 5.8. Calcd for $C_{22}H_{34}N_2O_2Sn$ (477.22): C, 55.37; H, 7.18; N, 5.87.

2: 2.03 g of *p-tert*-butylphenol; yield 1.29 g (65%); colorless crystals (from *n*-hexane); mp 149 °C. ^{1}H NMR (400.13 MHz, $CDCl_3$): 7.09 (m, 4H, *o*-Ph), 6.85 (m, 4H, *m*-Ph), 2.39 (s + m, 16H, NMe_2, NCH_2), 1.83 (m, 4H, CH_2), 1.47 (m, 4H, $SnCH_2$), 1.27 (s, 18H, *t*-Bu). ^{13}C NMR (62.93 MHz, CD_2Cl_2): 160.9 (C_i), 139.5 (C_p), 126.7 (C_m), 119.2 (C_o), 60.7 [$^3J(^{13}C-^{119/117}Sn)$ = 55] (NCH_2), 46.4 (NCH_3), 34.1 (CCH_3), 31.9 (CCH_3), 22.4 [$^2J(^{13}C-^{119/117}Sn)$ = 38] (CH_2), 17.9 [$^1J(^{13}C-^{119/117}Sn)$ = 829/791] ($SnCH_2$). ^{13}C CP-MAS NMR (100.6 MHz): 162.5, 138.1, 126.2, 119.1 (phenyl carbons), 60.7 (NCH_2), 48.4, 41.9 (NCH_3), 34.7 (CCH_3), 33.1 (CCH_3), 22.4 (CH_2), 18.0 ($SnCH_2$). ^{119}Sn NMR (111.92 MHz, $CHCl_3/D_2O_{ext}$): −233.4. ^{117}Sn NMR (89.15 MHz, CD_2Cl_2): −240.8. ^{119}Sn CP-MAS NMR (149.21 MHz): −251.8. Mass spectrum: *m/e* 441 ($C_{20}H_{37}N_2OSn^+$, 100%), 355 ($C_{15}H_{25}NOSn^+$, 3%), 292 ($C_{10}H_{24}N_2Sn^+$, 3%), 269 ($C_{10}H_{13}OSn^+$, 3%), 206 ($C_5H_{12}NSn^+$, 26%), 84 ($C_5H_{12}N^+$, 68%). Anal. Found: C, 61.3; H, 8.4; N, 4.7. Calcd for $C_{30}H_{50}N_2O_2Sn$ (589.48): C, 61.13; H, 8.55; N, 4.75.

3: 1.87 g of *p*-nitrophenol; yield 1.15 g (60%); colorless crystals (from *n*-hexane/dichloromethane (2:1)); mp 192 °C. ^{1}H NMR (400.13 MHz, $CDCl_3$): 7.96 (d, 4H, *m*-Ph), 6.70 (d, 4H, *o*-Ph), 2.45 (s, 4H, NCH_2), 2.36 (s, 12H, NMe_2), 1.89 (s, 4H, CH_2), 1.52 (s, 4H, $SnCH_2$). ^{13}C NMR (62.93 MHz, CD_2Cl_2): 170.7 (C_i), 138.4 (C_p), 126.5 (C_m), 119.6 (C_o), 60.3 [$^3J(^{13}C-^{119/117}Sn)$ = 64] (NCH_2), 46.2 (NCH_3), 22.1 [$^2J(^{13}C-^{119/117}Sn)$ = 42] (CH_2), 19.4 [$^1J(^{13}C-^{119/117}Sn)$ = 862/816] ($SnCH_2$). ^{13}C CP-MAS NMR (100.6 MHz): 172.1, 138.7, 126.4, 121.0 (phenyl carbons), 56.4 (NCH_2), 44.9 (NCH_3), 21.3 (CH_2), 18.2 ($SnCH_2$). ^{119}Sn NMR (111.92 MHz, $CHCl_3/D_2O_{ext}$): −271.1. ^{119}Sn CP-MAS NMR (149.22 MHz): − 279.1. Mass spectrum: *m/e* 430 ($C_{16}H_{28}N_3O_3Sn^+$, 21%), 378 ($C_{12}H_8N_2O_5Sn^+$, 5%), 206 ($C_5H_{12}NSn^+$, 26%), 139 ($C_6H_4NO_3Sn^+$, 40%), 84 ($C_5H_{12}N^+$, 50%). Anal. Found: C, 46.5; H, 5.7; N, 10.1. Calcd for $C_{22}H_{32}N_4O_6Sn$ (567.26): C, 46.58; H, 5.69; N, 9.88.

4: 1.51 g of 2-fluorophenol; yield 1.23 g (71%); colorless crystals (from *n*-hexane); mp 184 °C. ^{1}H NMR (400.13 MHz, $CDCl_3$): 7.03 (dd, 2H), 6.90 (dd, 2H), 6.77 (dd, 2H), 6.52 (d, 2H), 2.43 (t, 4H, NCH_2), 2.31 (s, 12H, NMe_2), 1.86 (q, 4H, CH_2), 1.49 (t, 4H, $SnCH_2$). ^{13}C NMR (62.93 MHz, CD_2Cl_2): 151.1 [$^2J(^{13}C-^{19}F)$ = 11 (C_1), 155.1 [$^1J(^{13}C-^{19}F)$ = 239 (C_2), 115.7 [$^2J(^{13}C-^{19}F)$ = 20 (C_3), 116.6 [$^4J(^{13}C-^{19}F)$ = 7 (C_5), 124.5 and 122.0 [$^3J(^{13}C-^{19}F)$ = 3 and $^3J(^{13}C-^{19}F)$ = 3 (C_4 and C_6), 60.4 [$^3J(^{13}C-^{119/117}Sn)$ = 62] (NCH_2), 46.1 (NCH_3), 22.2 [$^2J(^{13}C-^{119/117}Sn)$ = 40] (CH_2), 18.6 [$^1J(^{13}C-^{119/117}Sn)$ = 830/788] ($SnCH_2$). ^{13}C CP-MAS NMR (100.63 MHz): 156.8, 154.1, 152.0, 124.4, 122.7, 117.6 (phenyl carbons), 59.0 (NCH_2), 47.3, 43.0 (NCH_3), 22.9 (CH_2), 14.3 ($SnCH_2$). ^{119}Sn NMR (111.92 MHz, $CHCl_3/D_2O_{ext}$): −254.3. ^{117}Sn NMR (89.15 MHz, CD_2Cl_2): −253.9. ^{19}F NMR (235.35 MHz, CD_2Cl_2): −137.6. ^{119}Sn CP-MAS NMR 149.22 MHz): −259.7. Mass spectrum: *m/e* 403 ($C_{16}H_{28}N_2OFSn^+$, 87%), 317 ($C_{12}H_{16}NOFSn^+$, 2%), 206 ($C_5H_{12}NSn^+$, 53%), 84 ($C_5H_{12}N^+$, 68%). Anal. Found: C, 51.5; H, 6.4; N, 5.5. Calcd for $C_{22}H_{32}F_2N_2O_2Sn$ (513.19): C, 51.49; H, 6.28; N, 5.46.

Synthesis of the 2,2-Bis(3-(dimethylamino)propyl)-1,3-dioxa-2-stannaindane Derivatives (5, 6). A solution of bis-(3-(dimethylamino)propyl)diphenyltin (1.50 g, 3.37 mmol) and the corresponding catechol (3.37 mmol) in toluene was heated at reflux for 12 h. The reaction mixture turned dark violet. The toluene and the benzene formed during the reaction were removed under reduced pressure to leave a residue which was recrystallized from *n*-hexane to give violet crystals.

5: 0.37 g of catechol; yield 0.83 g (62%); mp 145 °C. ^{1}H NMR (400.13 MHz, $CDCl_3$): 6.63 (m, 2H), 6.40 (m, 2H), 2.43 (t, 4H, NCH_2), 2.27 (s, 12H, NMe_2), 1.85 (q, 4H, CH_2), 0.98 (t, 4H, $SnCH_2$). ^{13}C NMR (62.93 MHz, CD_2Cl_2): 154.6 (C_i), 116.2 (C_{m+p}), 113.8 [$^3J(^{13}C-^{119/117}Sn)$ = 28] (C_o), 60.3 [$^3J(^{13}C-^{119/117}Sn)$ = 63/60] (NCH_2), 45.2 (NCH_3), 22.1 [$^2J(^{13}C-^{119/117}Sn)$ = 36/34] (CH_2), 18.1 [$^1J(^{13}C-^{119/117}Sn)$ = 750/718] ($SnCH_2$). ^{13}C CP-MAS NMR (100.6 MHz): 155.9, 116.1, 112.7, 111.8 (phenyl carbons), 59.9 (NCH_2), 46.2 (NCH_3), 43.4 ($NCH3$), 22.1, 20.5, 17.5 (CH_2, $SnCH_2$). ^{119}Sn NMR (111.92 MHz, $CHCl_3/D_2O_{ext}$): −184.9. ^{119}Sn CP-MAS NMR (149.21 MHz): −185.5. Mass spectrum: *m/e* 400

(34) (a) Sheldrick, G. M. *Acta Crystallogr.* **1990** *A46*, 467. (b) Sheldrick, G. M. SHELXL97; University of Göttingen, Göttingen, Germany, 1997. (c) Flack, H. D. *Acta Crystallogr.* **1983**, *A39*, 876. (d) *International Tables for Crystallography*; Kluwer Academic: Dordrecht, The Netherlands, 1992; Vol. C. (e) Sheldrick, G. M., *SHELXTL Release 5.1 Software Reference Manual*; Bruker AXS: Madison, WI, 1997.

($C_{16}H_{28}N_2O_2Sn^+$, 40%), 314 ($C_{11}H_{16}NO_2Sn^+$, 2%), 228 ($C_6H_4O_2Sn^+$, 7%), 206 ($C_5H_{12}NSn^+$, 20%), 164 ($C_3H_8Sn^+$, 3%), 86 ($C_5H_{12}N^+$, 61%). Anal. Found: C, 48.2; H, 7.1; N, 7.0. Calcd for $C_{16}H_{28}N_2O_2Sn$ (399.09): C, 48.15; H, 7.07; N, 7.02.

6: 0.47 g of *o*-methoxycatechol; yield 1.05 g (73%); mp 159 °C. ^{1}H NMR (400.13 MHz, $CDCl_3$): 6.44−6.21 (aromatic protons), 3.80 (s, 3H, O−CH_3), 2.48 (t, 4H, NCH_2), 2.32 (s, 12H, NMe_2), 1.88 (q, 4H, CH_2), 1.08 (t, 4H, $SnCH_2$). ^{13}C NMR (62.93 MHz, CD_2Cl_2): 155.4 (C_1), 143.9 (C_2), 148.3 [$^3J(^{13}C-^{119/117}Sn)$ = 31] (C_3 = *C*−OCH_3), 103.5 (C_4), 114.4 (C_5), 108.8 [$^3J(^{13}C-^{119/117}Sn)$ = 28] (C_6), 60.4 [$^3J(^{13}C-^{119/117}Sn)$ = 63] (NCH_2), 56.9 (OCH_3), 45.2 (NCH_3), 22.1 [$^2J(^{13}C-^{119/117}Sn)$ = 35] (*C*H_2), 18.2 [$^1J(^{13}C-^{119/117}Sn)$ = 745/711] ($SnCH_2$). ^{13}C CP-MAS NMR (100.6 MHz): 156.8, 156.3, 147.5, 146.0, 116.0, 112.9, 111.6, 110.0 (phenyl carbons), 61.2, 59.6, 58.9 (NCH_2), 48.4, 47.1, 43.6, 42.8 (NCH_3), 21.7, 19.0 (*C*H_2), 17.1 ($SnCH_2$). ^{119}Sn NMR (111.92 MHz, $CHCl_3/D_2O_{ext}$): −179.7. ^{119}Sn CP-MAS NMR (149.21 MHz): −193.0, −199.8. Mass spectrum: *m/e* 430 ($C_{17}H_{30}N_2O_3Sn^+$, 100%), 344 ($C_{12}H_{18}NO_3Sn^+$, 3%), 258 ($C_7H_6O_3Sn^+$, 23%), 206 ($C_5H_{12}NSn^+$, 17%), 164 ($C_3H_8Sn^+$, 2%), 86 ($C_5H_{12}N^+$, 76%). Anal. Found: C, 47.6; H, 7.1; N, 6.5. Calcd for $C_{17}H_{30}N_2O_3Sn$ (427.17): C, 47.58; H, 7.05; N, 6.53.

Synthesis of Bis(3-(dimethylamino)propyl)tin Dithiophenolate (7). A mixture of bis(3-(dimethylamino)propyl)tin diphenolate (**1**; 0.50 g, 1.04 mmol) and thiophenol (0.34 g, 3.12 mmol) in toluene (25 mL) was heated at reflux for 12 h. The toluene and the excess thiophenol were distilled to give an oily residue, from which the phenol formed during the reaction was removed by Kugelrohr distillation. The residue was recrystallized from *n*-hexane to give **7** (0.43 g, 81%) as colorless crystals, mp 76 °C. ^{1}H NMR (400.13 MHz, $CDCl_3$): 7.48 (m, 4H, *o*-Ph), 7.13 (m, 6H, *m*,*p*-Ph), 2.21 (s, 12H, NMe_2), 2.17 (t, 4H, NCH_2), 1.67 (q, 4H, CH_2), 1.26 (t, 4H, $SnCH_2$). ^{13}C NMR (100.6 MHz, $CDCl_3$): 135.4 (C_i), 134.9 (C_o), 128.3 (C_m), 125.5 (C_p), 61.5 ($^3J(^{13}C-^{119/117}Sn)$ = 57, NCH_2), 45.9 (NCH_3), 22.7 ($^2J(^{13}C-^{119/117}Sn)$ = 33, *C*H_2), 18.3 ($^1J(^{13}C-^{119/117}Sn)$ = 520/497, $SnCH_2$). ^{13}C CP-MAS NMR (149.21 MHz): 139.2, 135.2, 129.0, 126.5 (phenyl carbons), 60.6 (NCH_2), 49.5 (NCH_3), 24.0 (*C*H_2), 19.6 ($SnCH_2$). ^{117}Sn NMR (186.50 MHz, C_7D_8): −1.7 ($^1J(^{117}Sn-^{13}C)$ = 493 Hz). ^{119}Sn CP-MAS NMR (149.21 MHz): − 37.3 ppm. Mass spectrum: *m/e* 423 ($C_{17}H_{22}NS_2Sn^+$, 8%), 400 ($C_{16}H_{29}N_2SSn^+$, 33%), 314 ($C_{11}H_{17}NSSn^+$, 3%), 292 ($C_{10}H_{24}N_2Sn^+$, 2%), 229 ($C_6H_5S_2Sn^+$, 12%), 206 ($C_5H_{12}NSn^+$, 26%). Anal. Found: C, 52.1; H, 7.0; N, 5.5. Calcd for $C_{22}H_{34}N_2S_2Sn$ (509.39): C, 51.87; H, 6.73; N, 5.50.

Synthesis of Bis(3-(dimethylamino)propyl)phenyltin Iodide (8). Iodine (0.86 g, 3.37 mmol) was added with ice cooling to a stirred solution of bis(3-(dimethylamino)propyl)-diphenyltin (1.50 g, 3.37 mmol) in CH_2Cl_2. After 1 h the solvent and iodobenzene were removed under reduced pressure. The residue was recrystallized from hot *n*-hexane/CH_2Cl_2 (1:1). Bis(3-(dimethylamino)propyl) phenyltin iodide (**8**) was obtained as a colorless crystalline solid: yield 65%; mp 218 °C). ^{1}H NMR (400.13 MHz, $CDCl_3$): 1.74 (m, 2H, $SnCH_2$), 1.81 (s, 6H, NCH_3), 1.97 (m, 2H, $SnCH_2$), 2.32−2.53 (m, 4H,CH_2), 2.56 (s, 6H, NCH_3), 7.40−7.59 (m, 5H, aromatic protons). ^{13}C NMR (100.63 MHz, $CDCl_3$): 10.7 ($^1J(^{119/117}Sn-^{13}C)$ = 518/490; $SnCH_2$), 21.8 ($^2J(^{119/117}Sn-^{13}C)$ = 33; CCH_2), 46.4/46.9 (NCH_3); 61.3 ($^3J(^{119/117}Sn-^{13}C)$ = 61, NCH_2); 138.0 (C_i); 135.2 ($^2J(^{13}C-^{119/117}Sn)$ = 39, C_o); 129.0 ($^3J(^{13}C-^{119/117}Sn)$ = 51, C_m); 129.3 (C_p). ^{13}C CP-MAS NMR (100.63 MHz): 141.4, 137.2, 135.6, 133.0, 131.7, 129.5 (phenyl carbons), 62.9, 60.2 (NCH_2), 50.3, 48.9, 46.2, 45.0 (NCH_3), 23.1, 21.2 (*C*H_2), 9.95 ($SnCH_2$). ^{119}Sn NMR (149.21 MHz, $CDCl_3$): −9.2. ^{119}Sn CP-MAS NMR (149.21 MHz): −6.3. Mass spectrum: *m/e* 410 ($C_{11}H_{17}NSnI^+$, 18%), 369 ($C_{16}H_{29}N_2Sn^+$, 35%), 284 ($C_{11}H_{17}NSn^+$, 9%), 206 ($C_5H_{12}NSn^+$, 4%). Molar conductivity (T = 20 °C): 2.55 S cm^2 mol^{-1} (CH_2Cl_2), 12.34 S cm^2 mol^{-1} (CH_3CN). Anal. Found: C, 38.7; H, 5.7; N, 5.7. Calcd for $C_{16}H_{29}N_2SnI$ (495.06): C, 38.82; H, 5.90; N, 5.66.

Acknowledgment. We thank the Deutsche Forschungsgemeinschaft, the Fonds der Chemischen Industrie, and the Martin Schmeisser Stiftung of Dortmund University for financial support (K.J., N.P., S.S., M.S.). The financial support of the Fund for Scientific Research, Flanders, Belgium (FWO, Grant No. G.0192.98) is gratefully acknowledged (R.W., M.B.). Partial financial support by the European Human and Capital Mobility Program, Contract No. ERBCHRX-CT94-0610, is acknowledged (K.J., R.W.). K.J. thanks B. Jousseaume and his colleagues for their great hospitality during a visiting professorship at the University of Bordeaux, Bordeaux, France, where a major part of this paper was written.

Supporting Information Available: Tables of all coordinates, anisotropic displacement parameters, and geometric data for compounds **1**−**8**. This material is available free of charge via the Internet at http://pubs.acs.org.

OM000813W